Report 2153

DEPARTMENT OF THE NAVY

HYDROMECHANICS

o

AERODYNAMICS

o

STRUCTURAL MECHANICS

o

APPLIED MATHEMATICS

o

ACOUSTICS AND VIBRATION

LONGITUDINAL AERODYNAMIC CHARACTERISTICS OF SEVERAL HYPERSONIC AIRCRAFT CONFIGURATIONS AT A MACH NUMBER OF 9.45

by

John R. Krouse and Bertram K. Ellis

AERODYNAMICS LABORATORY

RESEARCH AND DEVELOPMENT REPORT

Code 1

January 1966 Report 2153

LONGITUDINAL AERODYNAMIC CHARACTERISTICS OF SEVERAL HYPERSONIC AIRCRAFT CONFIGURATIONS AT A MACH NUMBER OF 9.45

by

John R. Krouse and Bertram K. Ellis

January 1966

Report 2153
Aero Report 1099

NOTATION

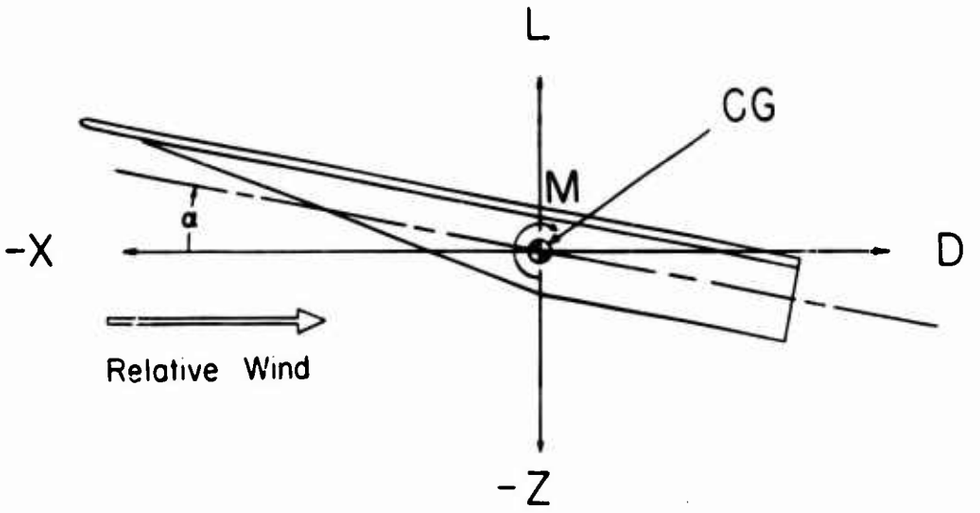

High Wing

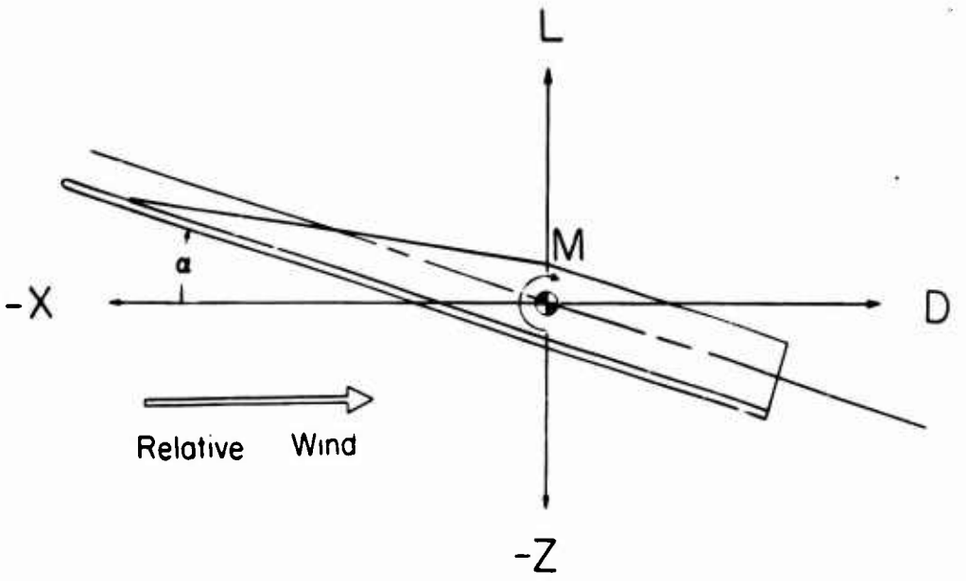

Low Wing

Axis	Force	Force Coefficient	Moment Coefficient
D (X)	D (drag)	$C_D = D/qS$	$C_m = M/qSc$
L (Z)	L (lift)	$C_L = L/qS$	

SYMBOLS

c	wing center-line chord, inches
c.p.	center of pressure (from wing apex), inches
C_D	drag coefficient
C_L	lift coefficient
C_m	pitching moment coefficient
D	drag, lb
L	lift, lb
L/D	lift-to-drag ratio
M	Mach number
p	pressure, psi
q	dynamic pressure, psi
Re	Reynolds number
S	projected wing area, in^2
T	temperature, ^oR
α	angle of attack, degrees
δ	wing-tip dihedral (positive, toward the fuselage), degrees

Subscripts

b	base of fuselage
t	stagnation conditions
∞	free-stream conditions

Configuration Identification Code

Wings:	W1 - Series 1 Wings (Straight Trailing Edges)
	W2 - Series 2 Wings (Extended Trailing Edges)
Bodies:	B1 - Low-Volume Fuselage
	B2 - High-Volume Fuselage

TABLE OF CONTENTS

	Page
NOTATION AND SYMBOLS	ii-iii
SUMMARY	1
INTRODUCTION	1
MODELS AND TEST APPARATUS	2
TEST CONDITIONS AND PROCEDURES	2
RESULTS AND DISCUSSION	3
AERODYNAMIC EFFICIENCY	4
LONGITUDINAL STATIC STABILITY	5
REFERENCES	7

LIST OF TABLES

Table 1 - Summary of Longitudinal Static Stability Characteristics (High-Wing Configurations)	8
Table 2 - Summary of Longitudinal Static Stability Characteristics (Low-Wing Configurations)	9

LIST OF ILLUSTRATIONS

Figure 1 - Principal Dimensions of Wing Configurations	10
Figure 2 - Principal Dimensions of Fuselage Configurations	11
Figure 3 - Photographs of a Typical Wing-Body Configuration	12
Figure 4 - Surface Flow Visualization of Several High-Wing Configurations	13-15
Figure 5 - Variation of Lift Coefficient With Angle of Attack	16-17
Figure 6 - Variation of Drag Coefficient With Angle of Attack	18-19
Figure 7 - Effects of Body Volume and Vehicle Orientation on Aerodynamic Efficiency	20-21
Figure 8 - Effects of Wing-Tip Dihedral on Aerodynamic Efficiency	22-23
Figure 9 - Reynolds Number Effects for a Typical Flat-Plate Configuration	24-26
Figure 10 - Experimental and Theoretical Comparison of the Aerodynamic Efficiency of Two Flat-Plate, High-Wing Configurations	27

TABLE OF CONTENTS (Concluded)

LIST OF ILLUSTRATIONS (Concluded)

	Page
Figure 11 - Effects of Body Volume and Wing Planform on Pitching Moment Coefficient (High-Wing Configurations)	28-30
Figure 12 - Effects of Body Volume and Wing Planform on Pitching Moment Coefficient (Low-Wing Configurations)	31-33
Figure 13 - Effects of Wing-Tip Dihedral and Vehicle Orientation on Pitching Moment Coefficient	34-37
Figure 14 - Variation of Center of Pressure With Angle of Attack	38-39

SUMMARY

Wind-tunnel tests were conducted at a Mach number of 9.45 to determine the longitudinal aerodynamic characteristics of several conceptual hypersonic aircraft configurations, consisting of various half-cone–cylinder bodies and double-delta wings. Effects of body volume, vehicle orientation, wing planform, and wing-tip dihedral were determined. In general, the lift-to-drag ratios of all high-wing configurations varied slightly over an angle-of-attack range of 0° to 12°, reaching maximum values of 2.7 around 6°. On the other hand, the lift-to-drag ratios of all low-wing configurations increased continuously with increasing angle of attack, eventually reaching maximum values of roughly 3.0 near 12°. In all cases, fuselage base drag accounted for less than 4 percent of the total drag. For the arbitrarily chosen center-of-gravity location, all low-wing configurations were unstable, unbalanced, or both; whereas several high-wing configurations were both stable and balanced.

INTRODUCTION

Several recent studies (References 1 through 4) have indicated that hypersonic cruise aircraft will probably require an air-breathing propulsion system utilizing liquid hydrogen fuel in order to obtain adequate range-payload performance characteristics. As a result of the very low density of this fuel (less than one-tenth that of conventional hydrocarbons), hypersonic aircraft will be characterized by very large fuselages necessary to contain an adequate supply of this high-energy propellant. The present investigation was undertaken to determine the longitudinal aerodynamic characteristics of several wing-body configurations, compatible with the aforementioned requirements and the general design philosophy discussed in Reference 5. The tests were performed in the Open-Jet Hypersonic Wind Tunnel of the David Taylor Model Basin Aerodynamics Laboratory at a Mach number of 9.45 and a unit Reynolds number of approximately 7.2×10^4 per inch. The results are presented herein.

MODELS AND TEST APPARATUS

The models consisted of two families of double-delta wings with cylindrically blunted leading edges and two half-cone–cylinder fuselages. One family of wings had straight trailing edges, and the other had extended trailing edges; both series of wings had wing-tip dihedral of 0° and 45° and a constant thickness equal to 1.25 percent of the wing centerline-chord (Figure 1). Positive and negative dihedral were obtained by mounting the wing so that the wing-tip deflection was toward or away from the fuselage, respectively. Both bodies had the same length but different maximum diameters (Figure 2). The wings and bodies were machined from stainless steel, and were completely interchangeable. A typical complete wing-body configuration is shown in Figure 3.

Force data were obtained with a Task Corporation, six-component, internal strain-gage balance. Data readout was acquired with a Beckman 210 solid-state system, which senses, measures, digitizes, and records the test data on magnetic tape for direct entry into an IBM 7090 computer. Fuselage base pressure was measured with a Pace 0 - 0.3 psid transducer. The data repeatability was as follows:

C_L	±0.002	L/D	±0.05
C_D	±0.002	M	±0.05
C_m	±0.0001	c.p. . . .	±0.03 in.

TEST CONDITIONS AND PROCEDURES

All tests were conducted under the following free-stream conditions:

	Average	Maximum	Minimum
p_∞, psi	0.0148	0.0150	0.0146
T_∞, °R	91.20	92.88	90.30
q_∞, psi	0.928	0.939	0.910
M	9.45	9.55	9.30
Re, per inch	71,800	75,700	67,600

All possible wing-body combinations were tested by varying the angle of attack of the model between limits of $\pm 12^\circ$ at a constant rate of one degree per second, while simultaneously obtaining continuous data during wind-tunnel operation. Physically, the models were mounted in the wind tunnel with the wing on top of the body. For each run, the data for half the angular range (upward) were interpreted as representing a high-wing model at positive α, the other half (downward) representing a low-wing model also at positive α. Force and moment components were measured, from which the following quantities were computed: C_L, C_D, L/D, C_m, and c.p. Fuselage base pressure was measured behind the cylindrical afterbody, midway between the sting and outer edge of the body. One flat-plate configuration (B1W1) was tested at a reduced Reynolds number of 48,600 per inch.

Surface flow visualization was obtained using ultraviolet light to excite a fluorescent pigment suspended in oil. The photographs which are shown in Figure 4 were taken through an overhead port during tunnel operation, using a Kodak yellow K2 filter mounted over a telephoto lens. An exposure time of four seconds was required with Polaroid N/P type film.

RESULTS AND DISCUSSION

Lift, drag, and pitching moment coefficients, aerodynamic efficiency, and center of pressure were obtained for all possible wing-body combinations for angles of attack up to 12°. Surface flow visualization photographs of several high-wing configurations (B1W2) were taken at angles of attack of 0°, 6°, and 12°. All coefficients are presented as a function of α (Figures 5 through 14), and are referenced to the projected wing area and wing center-line chord. The axis system, force and pitching moment coefficients, and configuration identification code are defined in the notation and symbols. The effects of body volume, vehicle orientation (high-wing or low-wing), wing planform, and wing-tip dihedral are discussed in the following paragraphs. Reynolds number effects are also presented for a typical flat-plate configuration (B1W1) and a comparison is made between the experimental results and theoretical calculations of the aerodynamic efficiency for two representative high-wing, flat-plate configurations (B1W1 and B2W2).

AERODYNAMIC EFFICIENCY

For the high-wing configurations, the lift-to-drag ratio was positive at an angle of attack of 0°, reached a maximum value of approximately 2.7 around $\alpha = 6°$, and decreased slightly thereafter. For the low-wing configurations, on the other hand, the lift-to-drag ratio was negative at an angle of attack of 0°, but it increased with increasing α, to a maximum value of roughly 3.0 near $\alpha = 12°$ (Figure 7).

The lift-to-drag ratios of the configurations with the small (B1) fuselage were higher than the corresponding configurations with the large (B2) fuselage over most of the angle-of-attack range (Figure 7). The wing planform, however, had little effect on the aerodynamic efficiency. In all cases, the base drag accounted for less than four percent of the total drag.

Deflecting the wing tips of the high-wing configurations into the relative wind ($\delta = 45°$) increased the aerodynamic efficiency except at the higher angles of attack (Figure 8a). On the low-wing configurations, deflecting the wing tips into the relative wind ($\delta = -45°$, in this case) gave higher L/D ratios than the configurations without dihedral up to $\alpha = 7°$, approximately. Negative dihedral was also superior to positive dihedral up to $\alpha = 9°$, approximately (Figure 8b).

Decreasing the Reynolds number had a detrimental effect on the lift-to-drag ratio of the B1W1 high-wing configuration for $0° < \alpha < 7°$; but for the corresponding low-wing configuration, decreasing Reynolds number had a slightly beneficial effect on L/D for $0° < \alpha < 3.5°$ and a fairly adverse effect for $3.5° < \alpha < 7°$ (Figure 9). Unfortunately, experimental data at the reduced Reynolds number could not be obtained at $\alpha > 7°$ because of flow breakdown in the open-jet test section.

Newtonian impact theory was used to calculate the lift-to-drag ratio of two flat-plate, high-wing configurations; namely, B1W1 and B2W2. The pertinent equations were obtained or derived from Reference 6. Each complete wing-body configuration was considered as three component parts: (1) half-cone forebody, (2) half-cylinder afterbody, and (3) wing. The coefficients were corrected to a common reference area (the exposed wing area) and then added for each component part to obtain the total coefficients of a complete wing-body configuration. Initial computations, neglecting wing

thickness, produced fairly poor correlation with the experimental data (Figure 10). Including the drag of the cylindrically blunted wing leading edge gave considerably better agreement. A further attempt was made to improve the results by accounting for skin-friction drag. The following simplifying assumptions were made: (1) the total exposed wing-body area was treated as a flat plate, and (2) the skin-friction was considered independent of α. For a Reynolds number based on the wing center-line chord, the coefficient of friction (C_f) was obtained from Figure 3 of Reference 7 by extrapolation to the existing temperature ratio. Correcting this viscous drag coefficient to the common reference area and adding it to the impact drag gave lift-to-drag ratios that agreed very favorably with the experimental data over the entire angle-of-attack range.

LONGITUDINAL STATIC STABILITY

The longitudinal static stability characteristics are summarized in Tables 1 and 2. The evaluation of the various configurations, in terms of C_m, was based on a center of gravity located seven inches from the wing apex (63.6 percent of the wing center-line chord). The pitching moment coefficients of all configurations were computed about this c.g. location, even though it will vary slightly with different wing-body combinations. Nevertheless, the arbitrarily chosen c.g. position is believed to be fairly representative of a similarly designed, full-scale aircraft. Moving the center of gravity forward or aft will affect the stability characteristics accordingly, but the relative merits of the various configurations should remain unchanged.

The high-wing configurations with $\delta = -45^\circ$ were unstable and unbalanced (Figure 11). Of the remaining configurations, those with W2 wings were more stable than the corresponding configurations with W1 wings (Figures 11 and 12). All low-wing configurations were unstable, unbalanced, or both, whereas several high-wing configurations were both stable and balanced (Figure 13). Moreover, a few of these high-wing configurations were balanced at angles of attack corresponding to the maximum lift-to-drag ratio (Figure 8). The center of pressure was practically independent of

angle of attack for $4^\circ < \alpha < 12^\circ$ for all high-wing configurations and nearly independent of angle of attack for $8^\circ < \alpha < 12^\circ$ for all low-wing configurations (Figure 14).

Aerodynamics Laboratory
David Taylor Model Basin
Washington, D. C.
October 1965

REFERENCES

1. Loftin, Laurence K., Jr. Hypersonic Aircraft Technology. Langley, Va., Jul 1963. 9 p. illus. (National Aeronautics & Space Adm. presentation to Aeronautics Press Briefing, Wash., 25 Jul 1963)
2. Wall, Douglas E. A Study of Hypersonic Aircraft. Edwards, Calif., Apr 1964. 6 p. illus. (National Aeronautics & Space Adm. TM X-56001)
3. Syvertson, C. A. and David H. Dennis. Trends in High-Speed Atmospheric Flight. N. Y., Jul 1964. 10 p. illus. (American Institute of Aeronautics & Astronautics. Paper 64-514)
4. Gregory, Thomas J., Richard H. Petersen, and John A. Wyss. Performance Trade-Offs and Research Problems for Hypersonic Transports. N. Y., Aug 1964. [11] p. incl. illus. (American Institute of Aeronautics & Astronautics. Paper 64-605)
5. Krouse, John R. Determination of the Cruise Range of a Hydrogen-Fueled, Air-Breathing Hypersonic Aircraft. Wash., May 1965. 22 p. incl. illus. (David Taylor Model Basin. Aero Rpt. 1089. Rpt. 2010)
6. Truitt, Robert Wesley. Hypersonic Aerodynamics. N. Y., Ronald Press Co. [1959]. 462 p.
7. Lee, Dorothy B. and Maxime A. Faget. Charts Adapted From Van Driest's Turbulent Flat-Plate Theory for Determining Values of Turbulent Aerodynamic Friction and Heat-Transfer Coefficients. Wash., Oct 1956. 16 p. incl. illus. (National Advisory Committee for Aeronautics. TN 3811)

Table 1

Summary of Longitudinal Static Stability Characteristics

(High-Wing Configurations)

Body	Wing-Tip Dihedral	Stability Characteristics	Remarks
Series 1 Wings (Straight Trailing Edges)			
B1	$\delta = 0^\circ$	Stable and balanced	A
	$\delta = 45^\circ$	Stable and marginally balanced	NA
	$\delta = -45^\circ$	Unstable and unbalanced	NA
B2	$\delta = 0^\circ$	Stable and unbalanced	NA
	$\delta = 45^\circ$	Stable and balanced	A
	$\delta = -45^\circ$	Unstable and unbalanced	NA
Series 2 Wings (Extended Trailing Edges)			
B1	$\delta = 0^\circ$	Stable and balanced	A
	$\delta = 45^\circ$	Stable and marginally balanced	NA
	$\delta = -45^\circ$	Unstable and unbalanced	NA
B2	$\delta = 0^\circ$	Stable and balanced	A
	$\delta = 45^\circ$	Stable and marginally balanced	NA
	$\delta = -45^\circ$	Unstable and unbalanced	NA

A - Acceptable

NA - Not Acceptable

Table 2

Summary of Longitudinal Static Stability Characteristics

(Low-Wing Configurations)

Body	Wing-Tip Dihedral	Stability Characteristics	Remarks
Series 1 Wings (Straight Trailing Edges)			
B1	$\delta = 0^\circ$	Stable and unbalanced	NA
	$\delta = 45^\circ$	Marginally stable and marginally balanced	NA
	$\delta = -45^\circ$	Stable and unbalanced	NA
B2	$\delta = 0^\circ$	Stable and unbalanced	NA
	$\delta = 45^\circ$	Marginally stable and unbalanced	NA
	$\delta = -45^\circ$	Marginally stable and unbalanced	NA
Series 2 Wings (Extended Trailing Edges)			
B1	$\delta = 0^\circ$	Stable and unbalanced	NA
	$\delta = 45^\circ$	Stable and marginally balanced	NA
	$\delta = -45^\circ$	Stable and unbalanced	NA
B2	$\delta = 0^\circ$	Stable and unbalanced	NA
	$\delta = 45^\circ$	Stable and marginally balanced	NA
	$\delta = -45^\circ$	Marginally stable and unbalanced	NA

NA - Not Acceptable

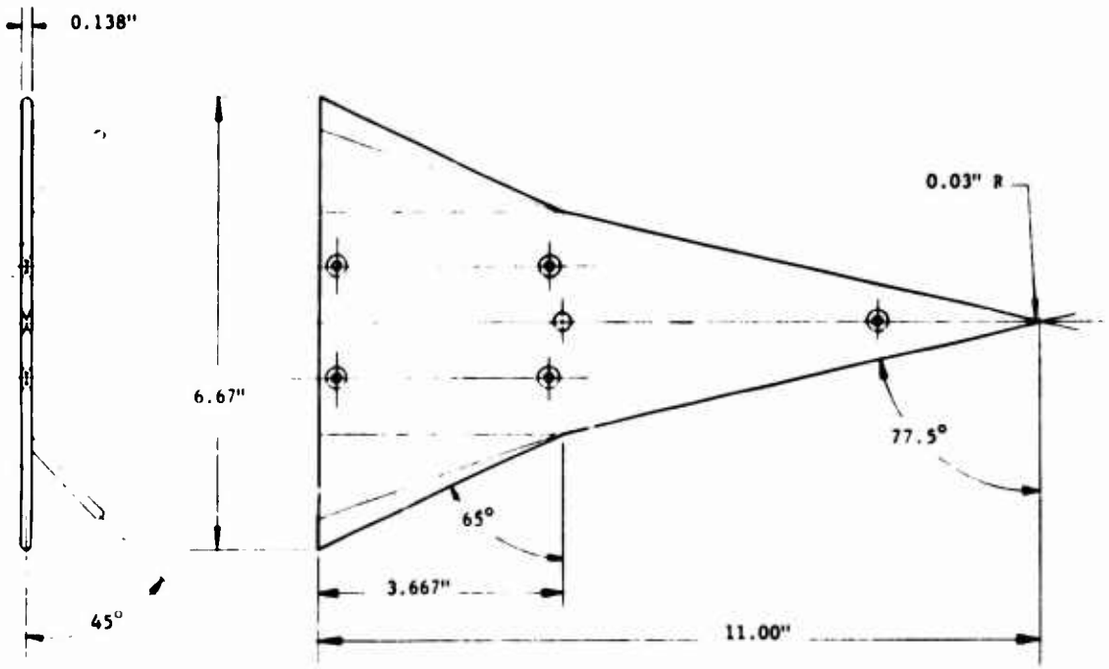

Series 1 Wings (Straight Trailing Edges)

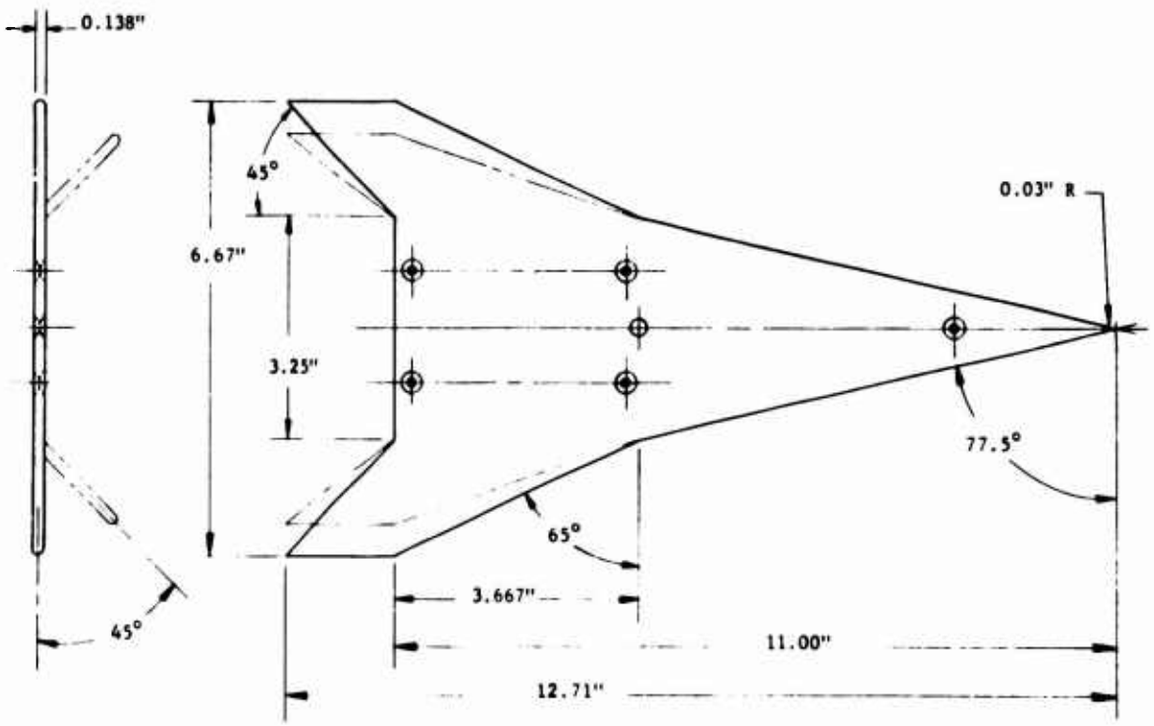

Series 2 Wings (Extended Trailing Edges)

Figure 1 - Principal Dimensions of Wing Configurations

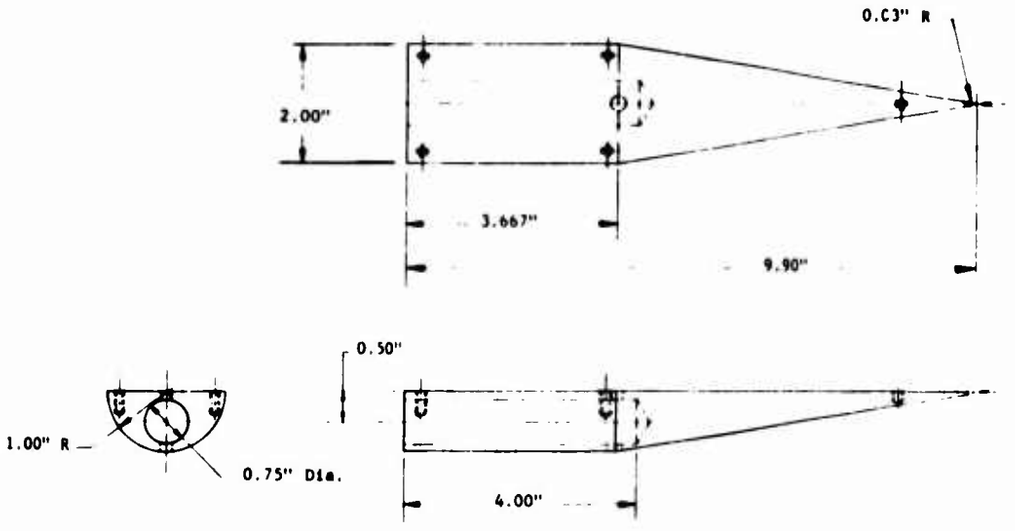

(a) Low-Volume Fuselage

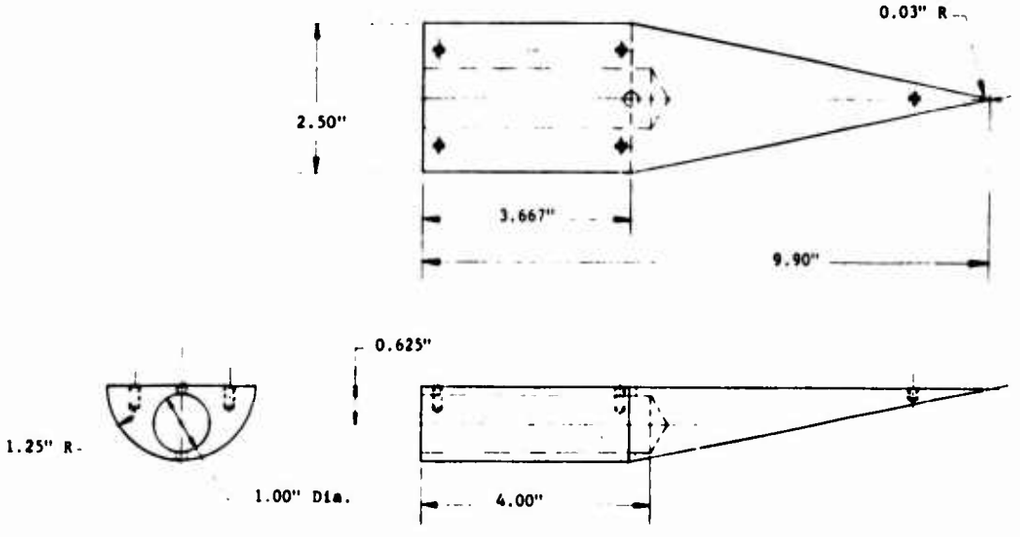

(b) High-Volume Fuselage

Figure 2 - Principal Dimensions of Fuselage Configurations

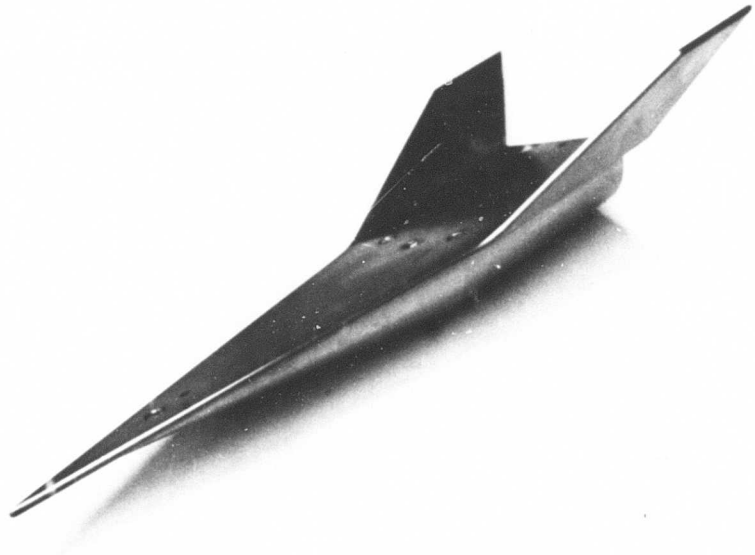

(a) High-Wing Configuration

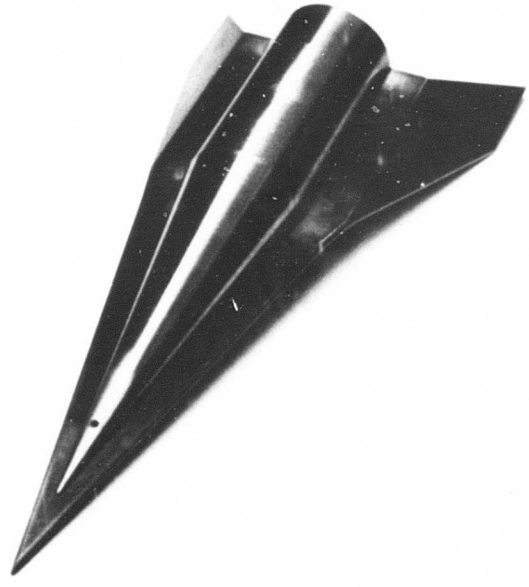

(b) Low-Wing Configuration

Figure 3 - Photographs of a Typical Wing-Body Configuration (B1W2 ; $\delta = -45^{\circ}$)

$\alpha = 12^\circ$

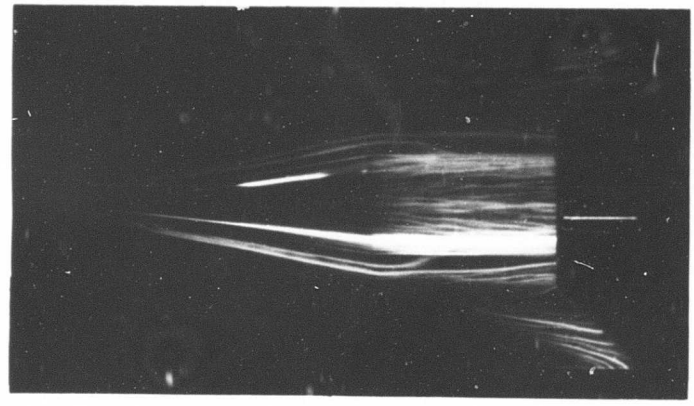

$\alpha = 6^\circ$

$\alpha = 0^\circ$

Figure 4 - Surface Flow Visualization of Several High-Wing Configurations (B1W2)

(a) $\delta = 0^\circ$

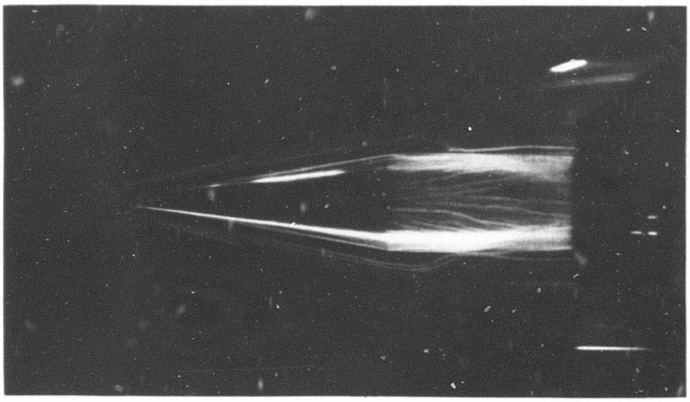

$\alpha = 12^\circ$

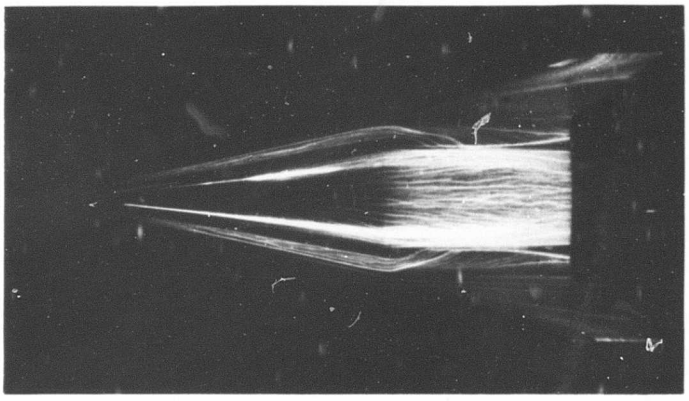

$\alpha = 6^\circ$

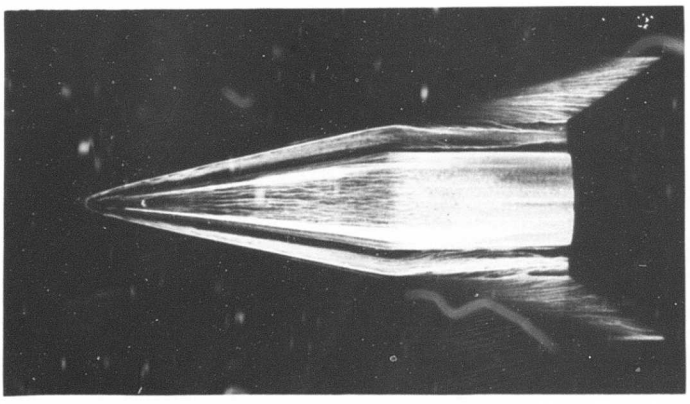

$\alpha = 0^\circ$

Figure 4 (Continued)

(b) $\delta = +45^\circ$

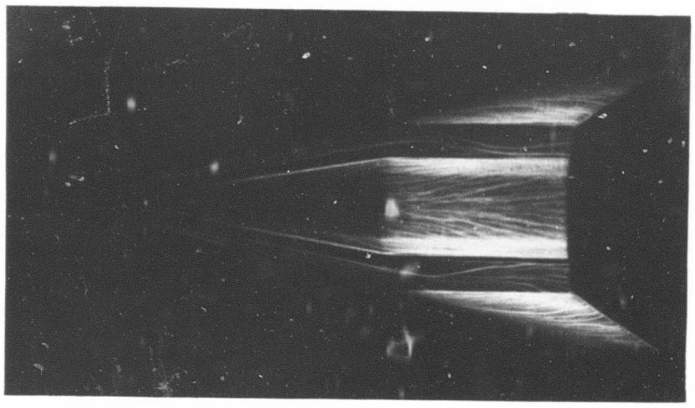

$\alpha = 12^\circ$

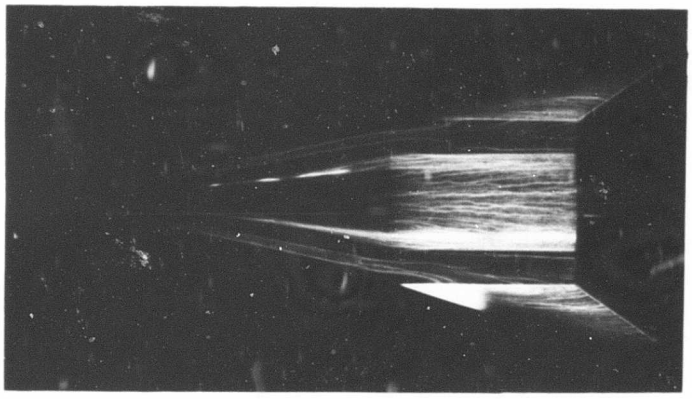

$\alpha = 6^\circ$

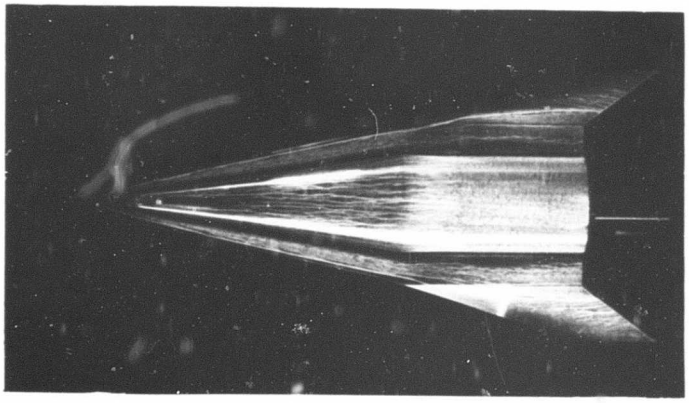

$\alpha = 0^\circ$

Figure 4 (Concluded)

(c) $\delta = -45^\circ$

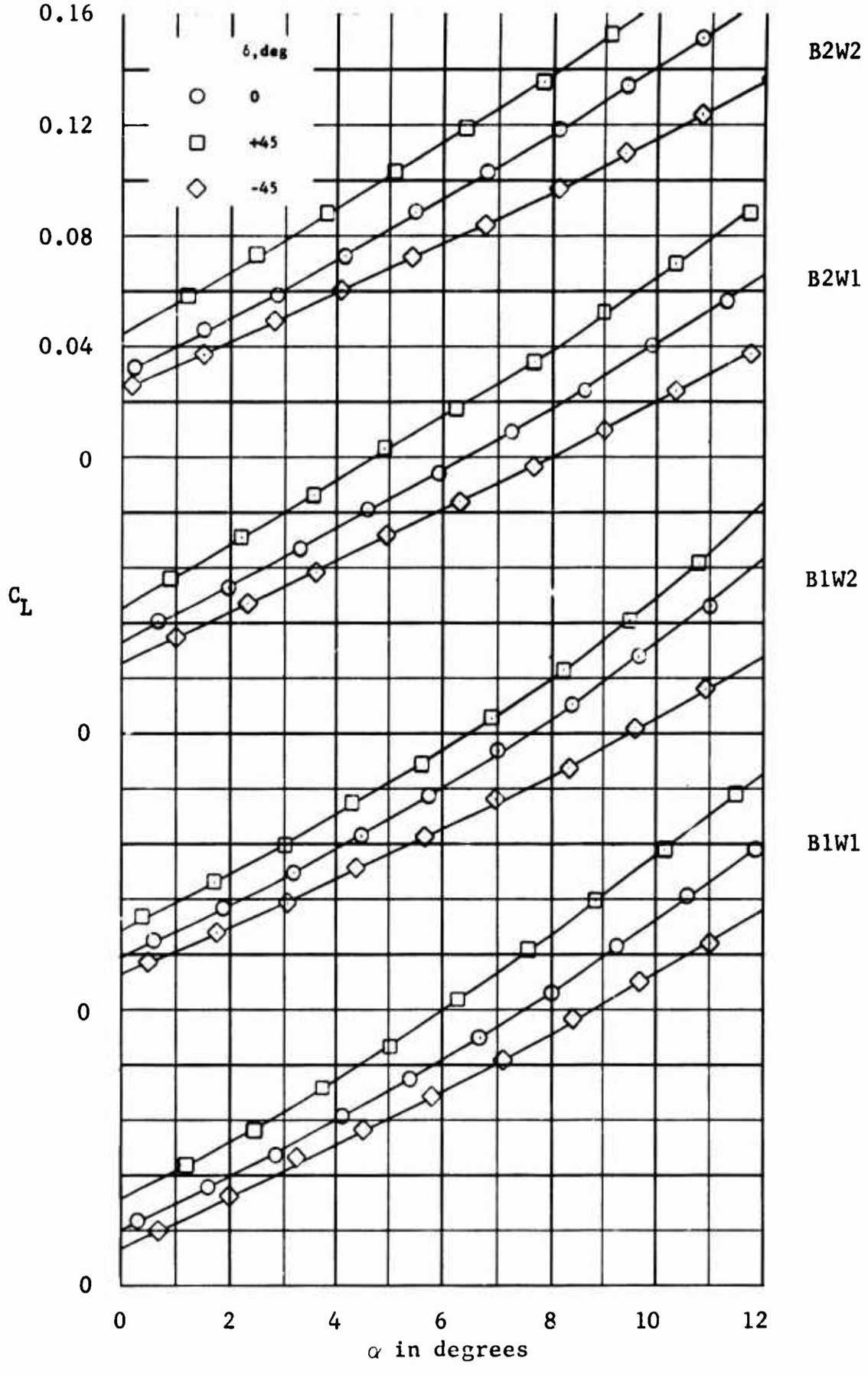

Figure 5 - Variation of Lift Coefficient with Angle of Attack

(a) High-Wing Configurations

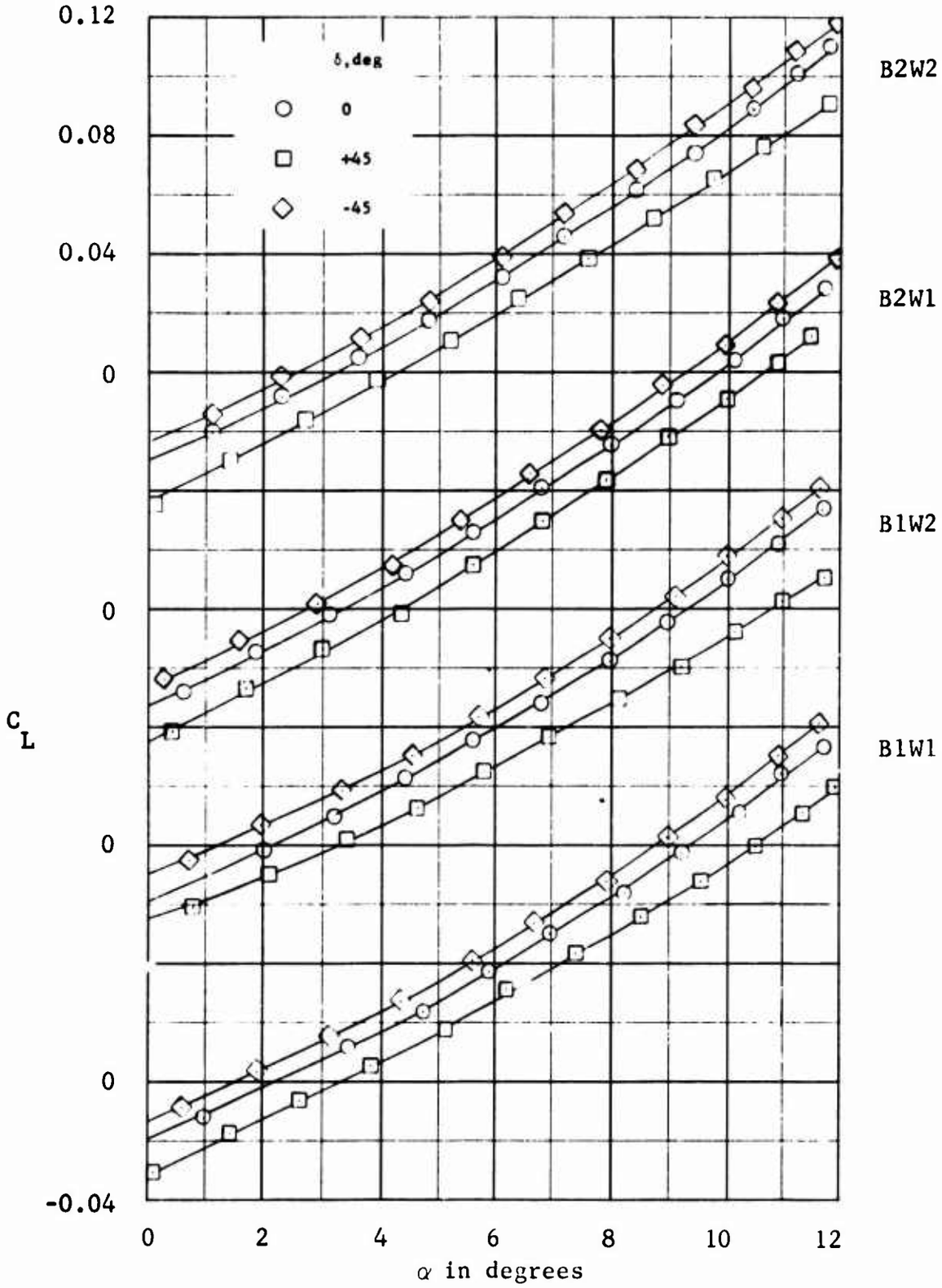

Figure 5 (Concluded)

(b) Low-Wing Configurations

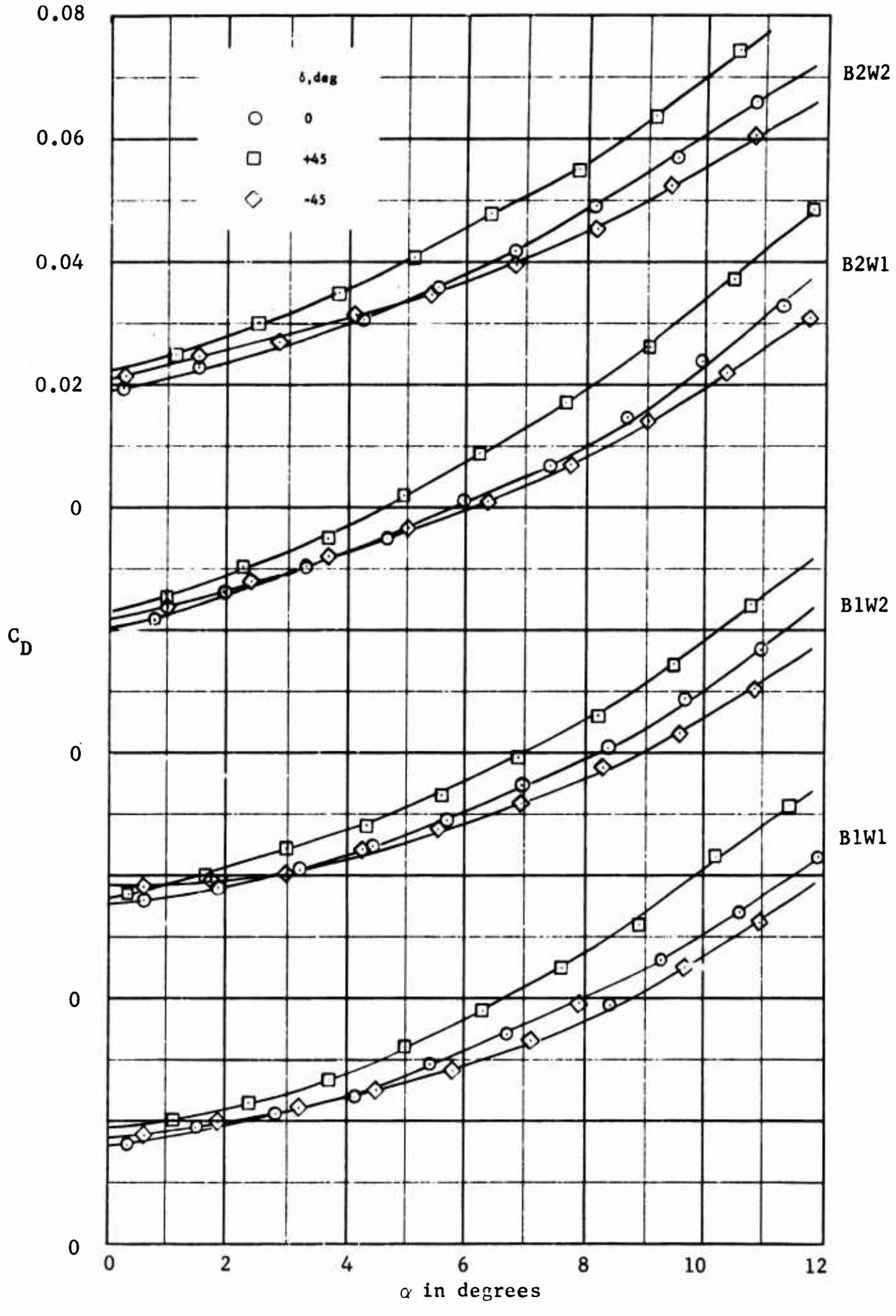

Figure 6 - Variation of Drag Coefficient with Angle of Attack
(a) High-Wing Configurations

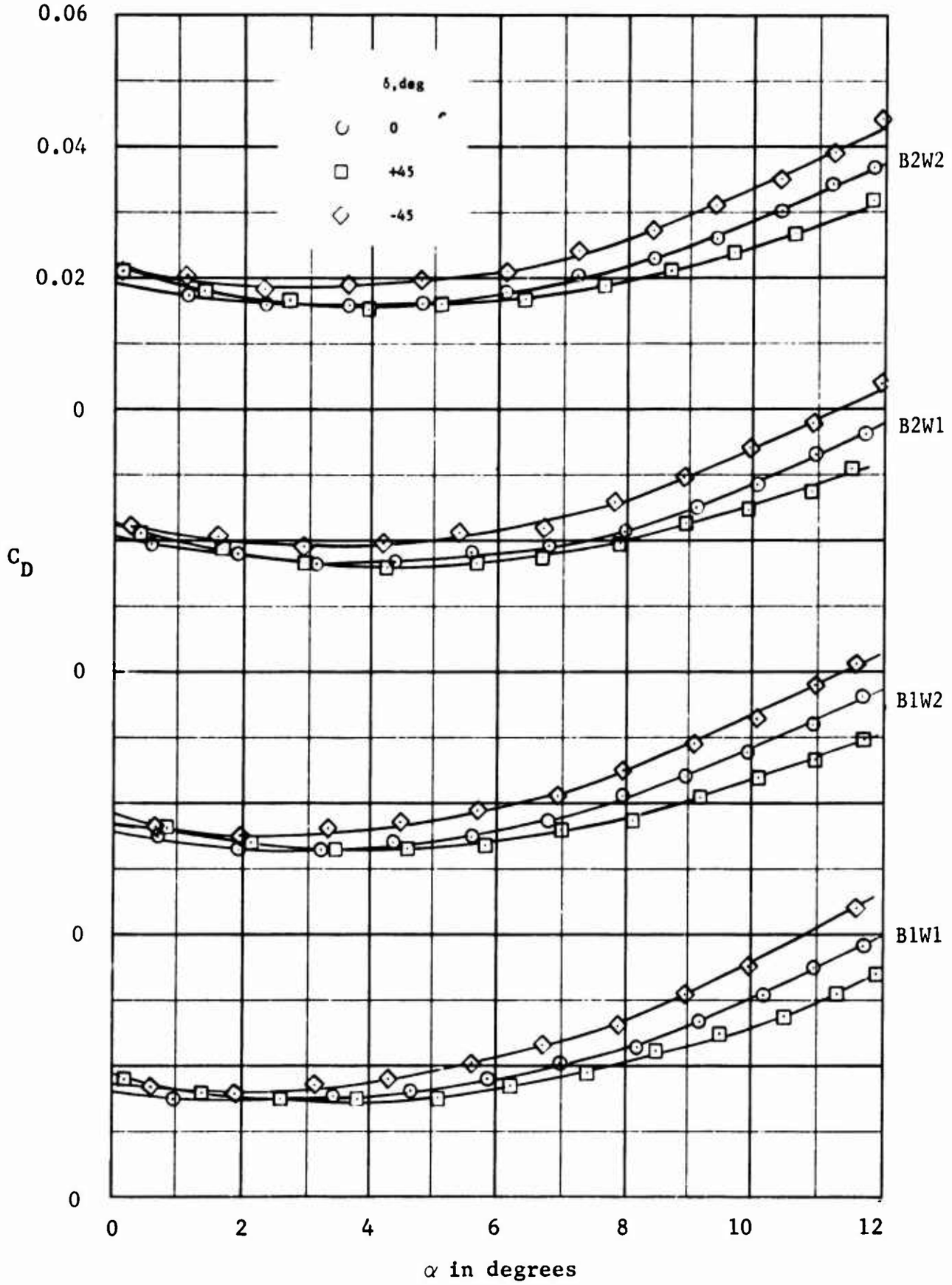

Figure 6 (Concluded)

(b) Low-Wing Configurations

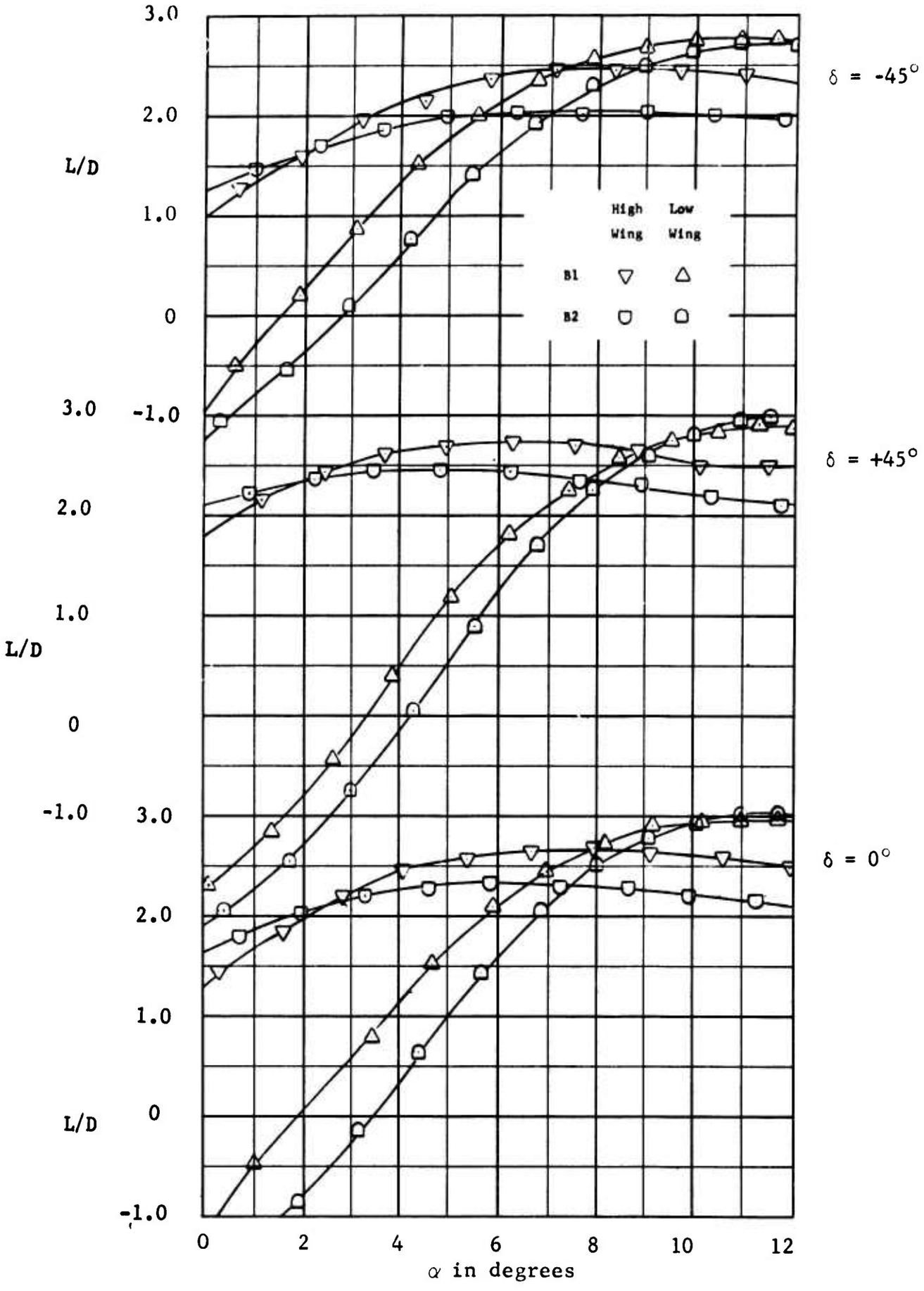

Figure 7 - Effects of Body Volume and Vehicle Orientation on Aerodynamic Efficiency
(a) Series 1 Wings

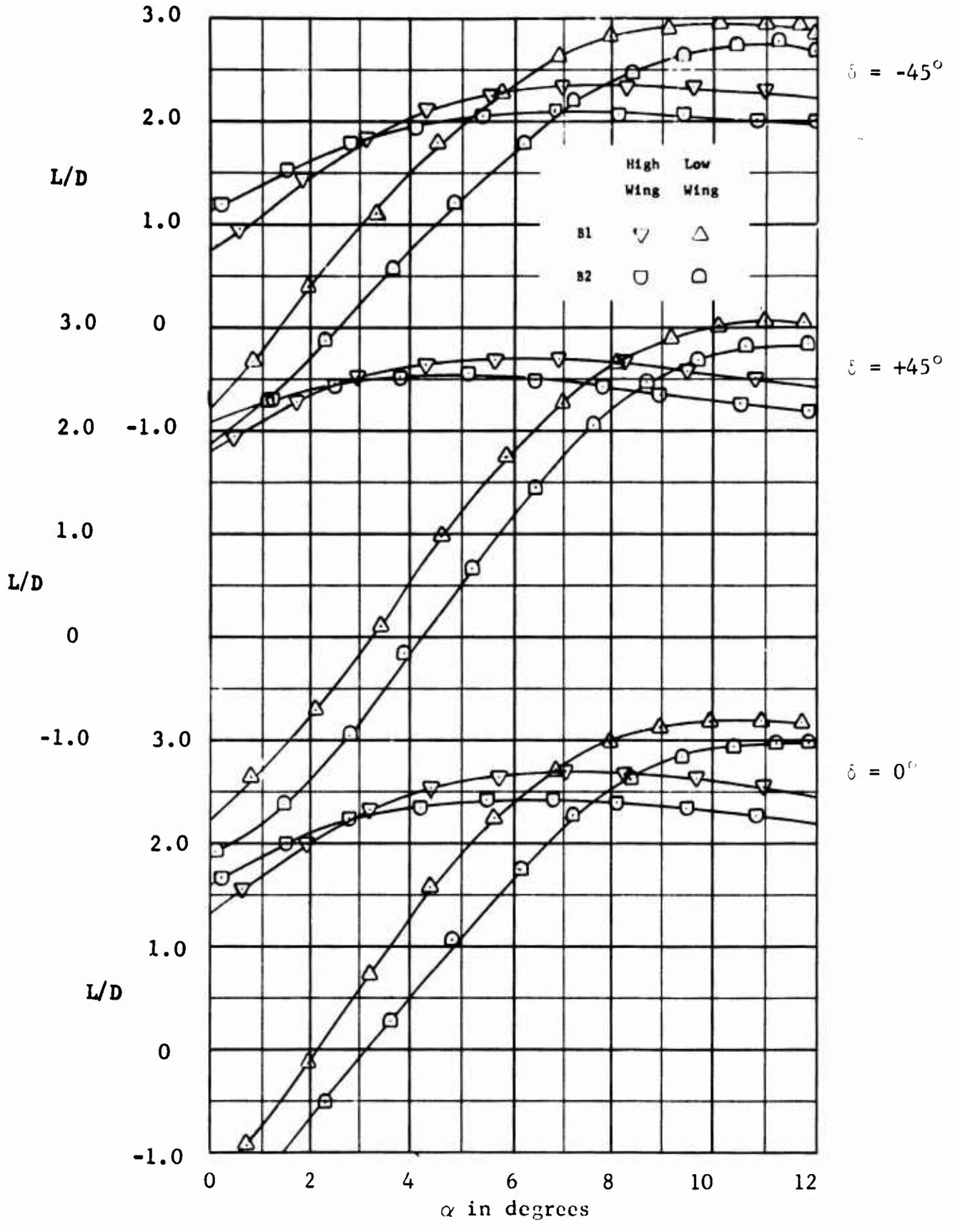

Figure 7 (Concluded)

(b) Series 2 Wings

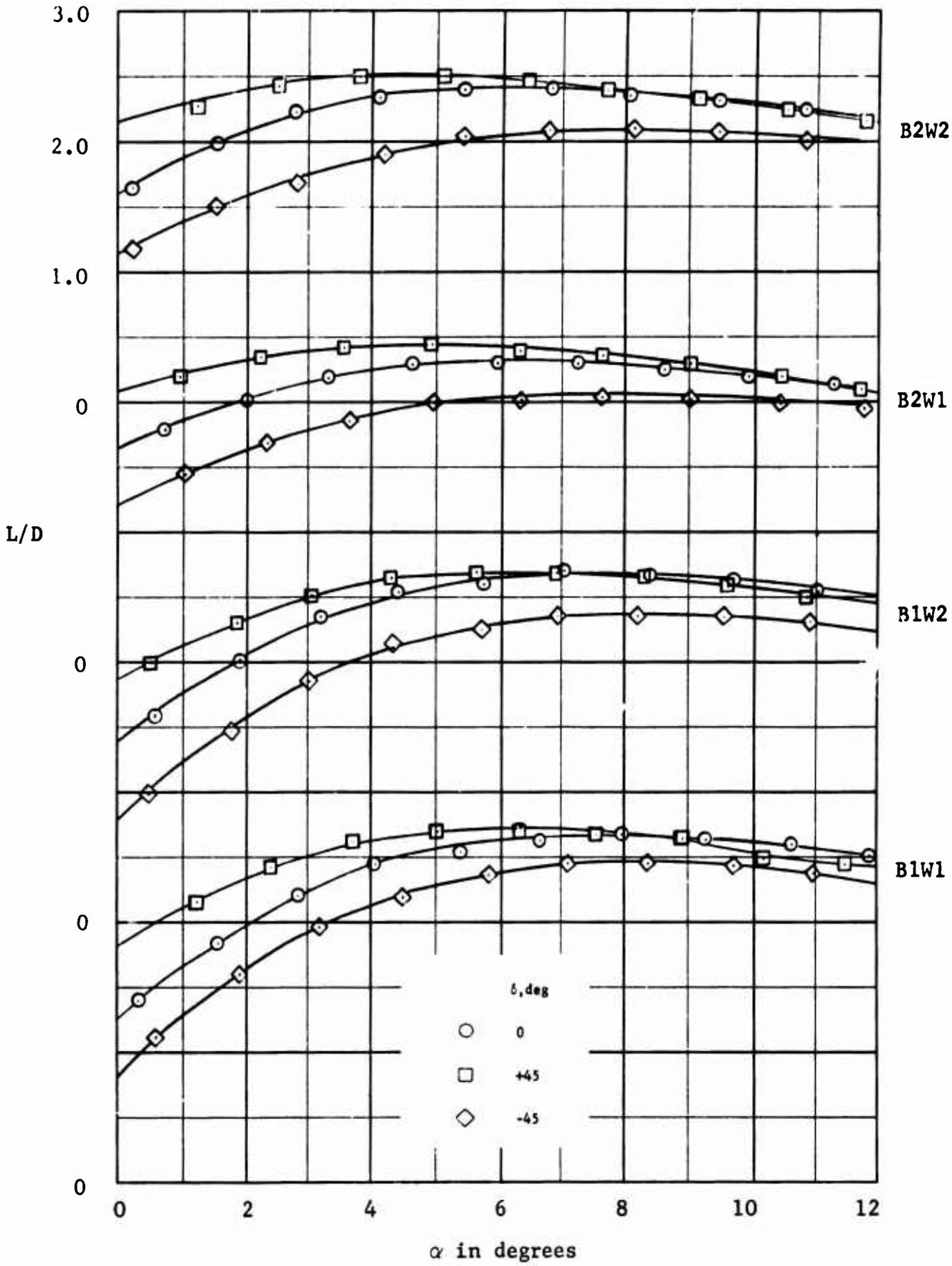

Figure 8 - Effects of Wing-Tip Dihedral on Aerodynamic Efficiency

(a) High-Wing Configurations

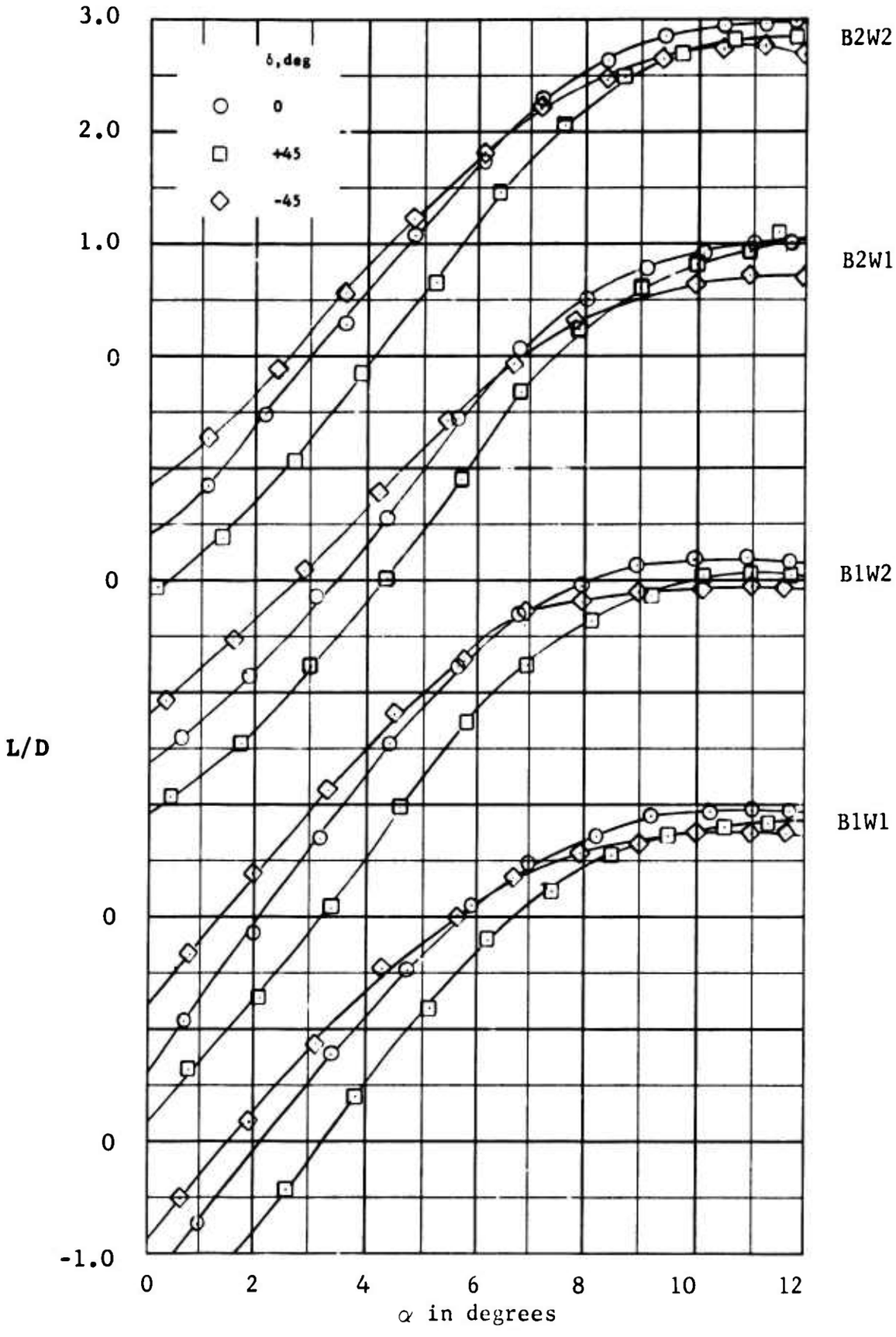

Figure 8 (Concluded)

(b) Low-Wing Configurations

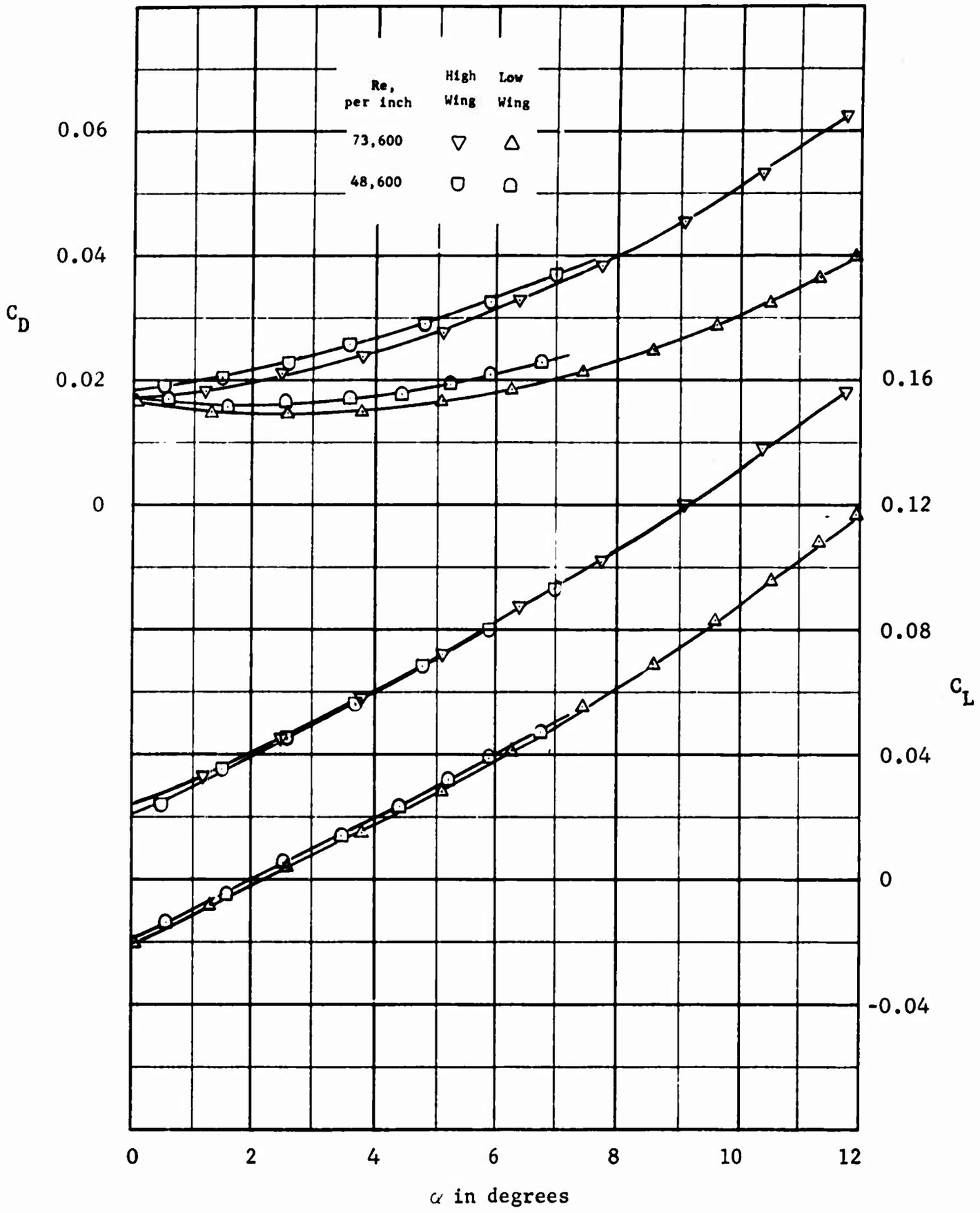

Figure 9 - Reynolds Number Effects for a Typical Flat-Plate Configuration (B1W1)

(a) Lift and Drag

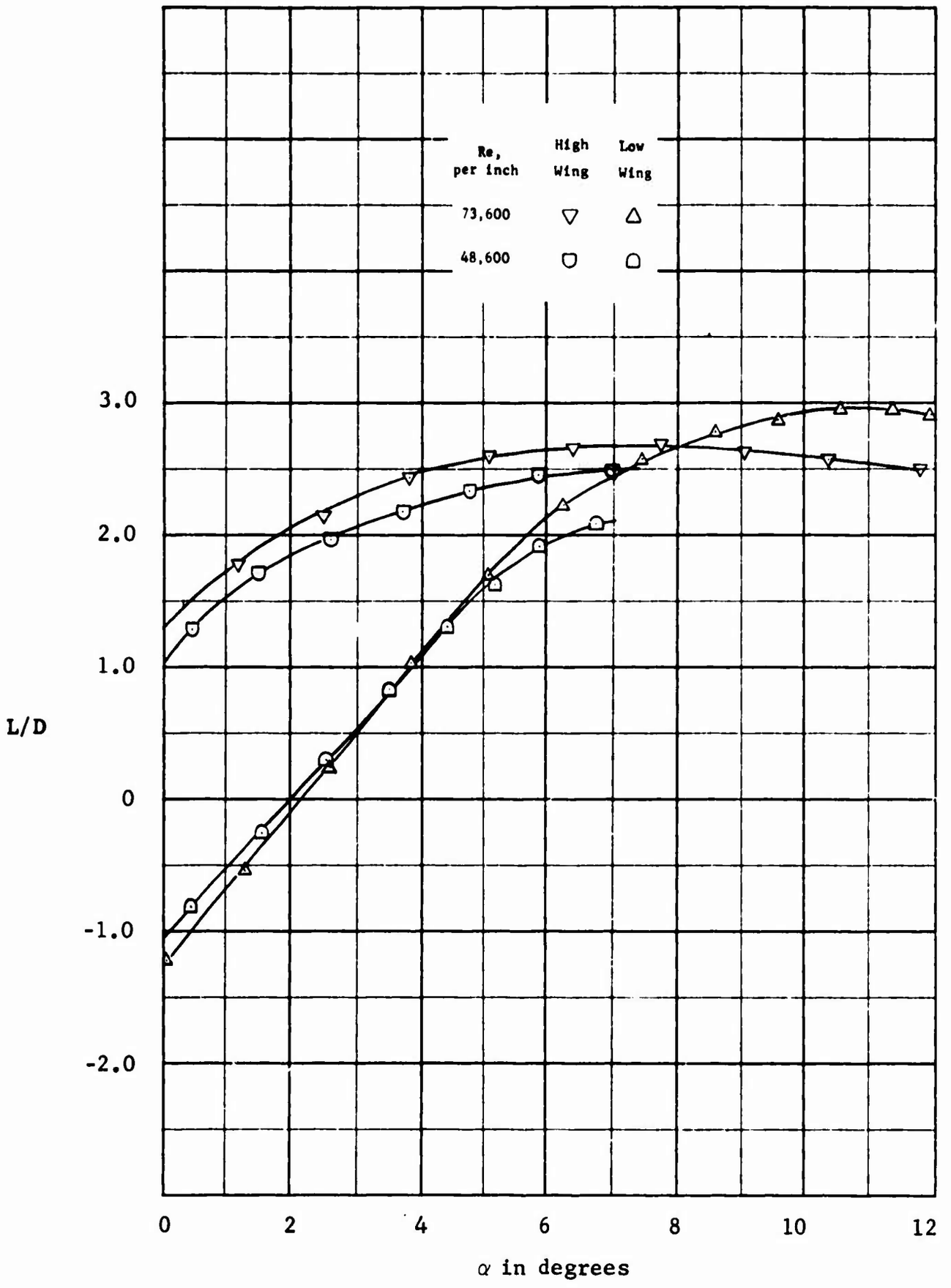

Figure 9 (Continued)

(b) Aerodynamic Efficiency

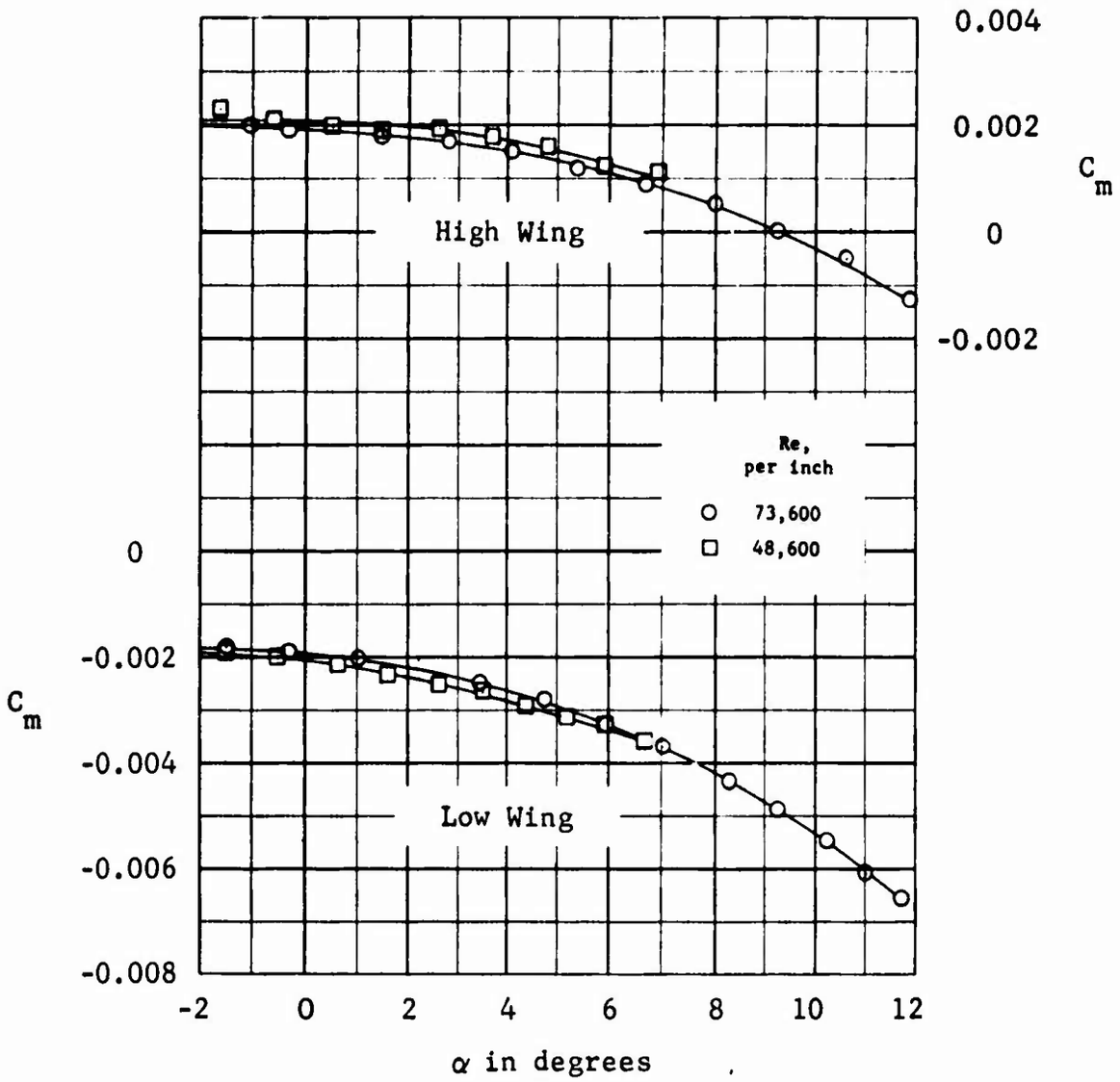

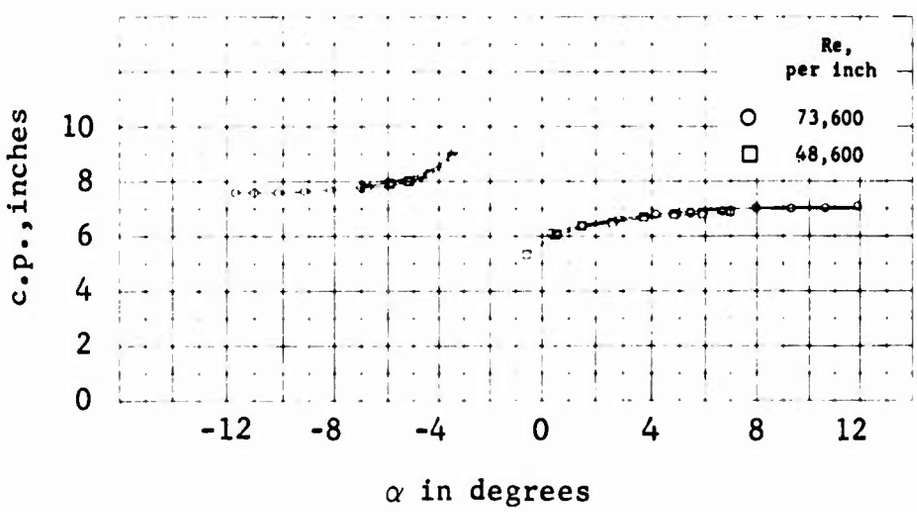

Figure 9 (Concluded)

(c) Pitching Moment Coefficient and Center of Pressure

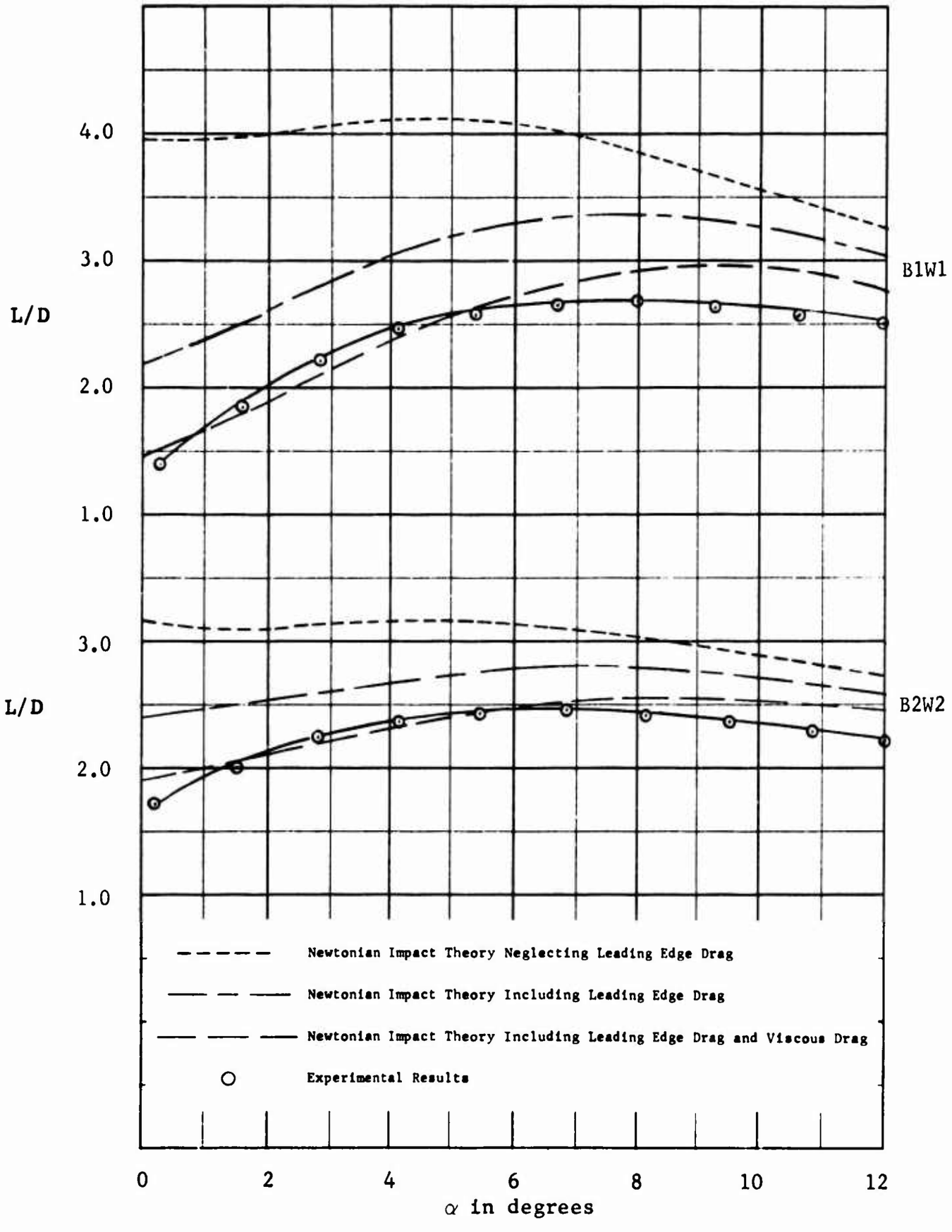

Figure 10 - Experimental and Theoretical Comparison of the Aerodynamic Efficiency of Two Flat-Plate, High-Wing Configurations

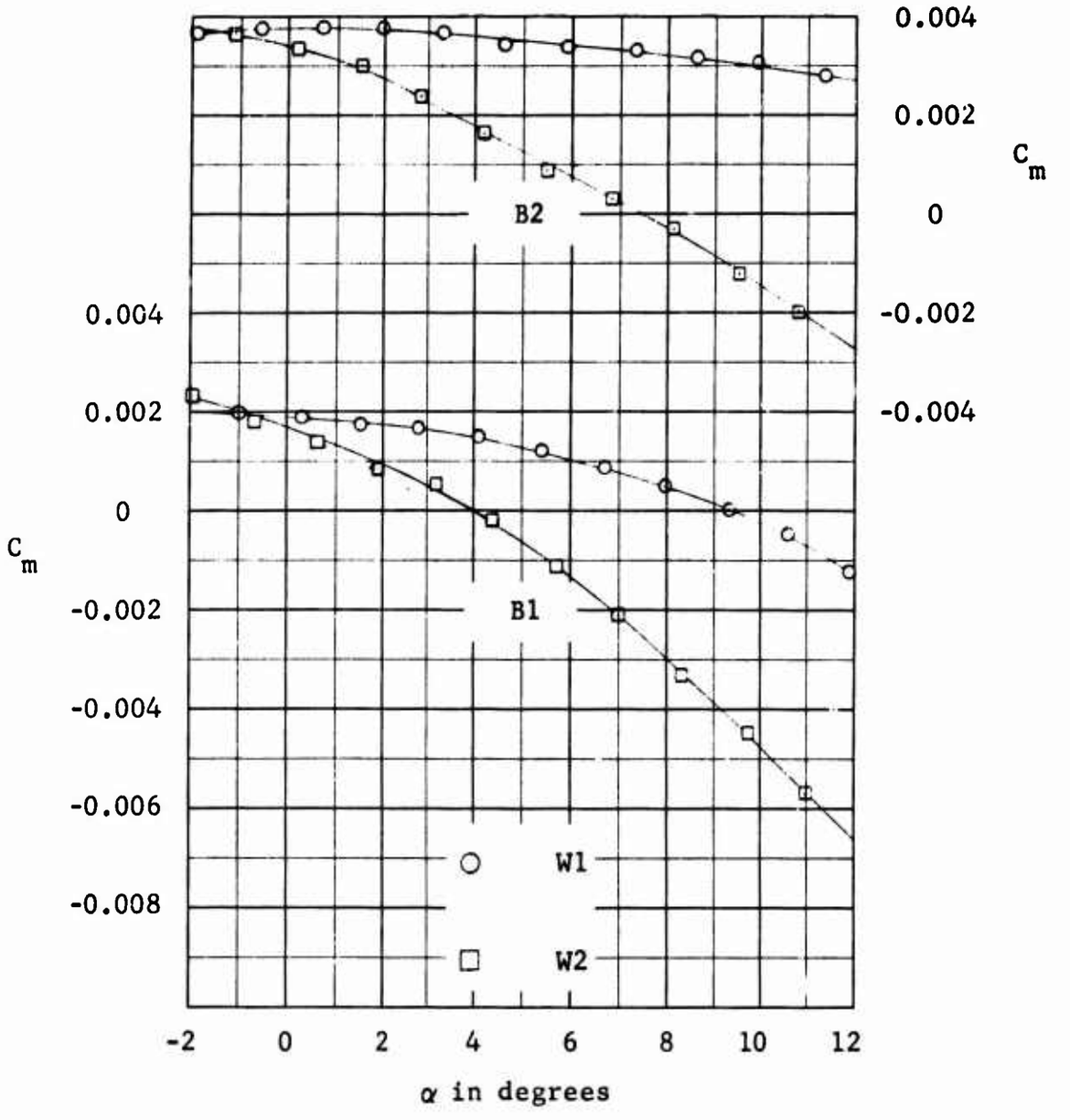

Figure 11 - Effects of Body Volume and Wing Planform on Pitching Moment Coefficient (High-Wing Configurations)

(a) $\delta = 0°$

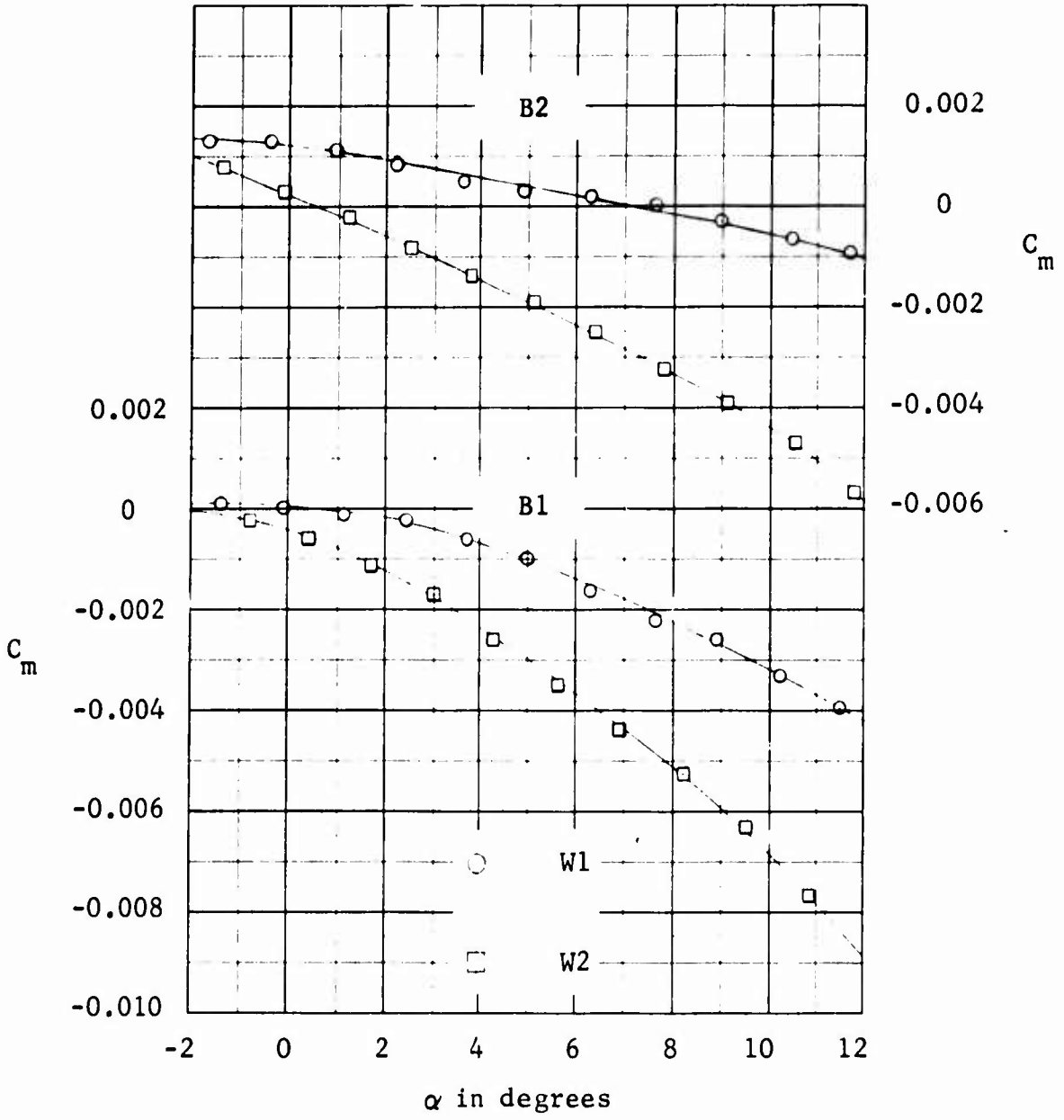

Figure 11 (Continued)

(b) $\delta = 45°$

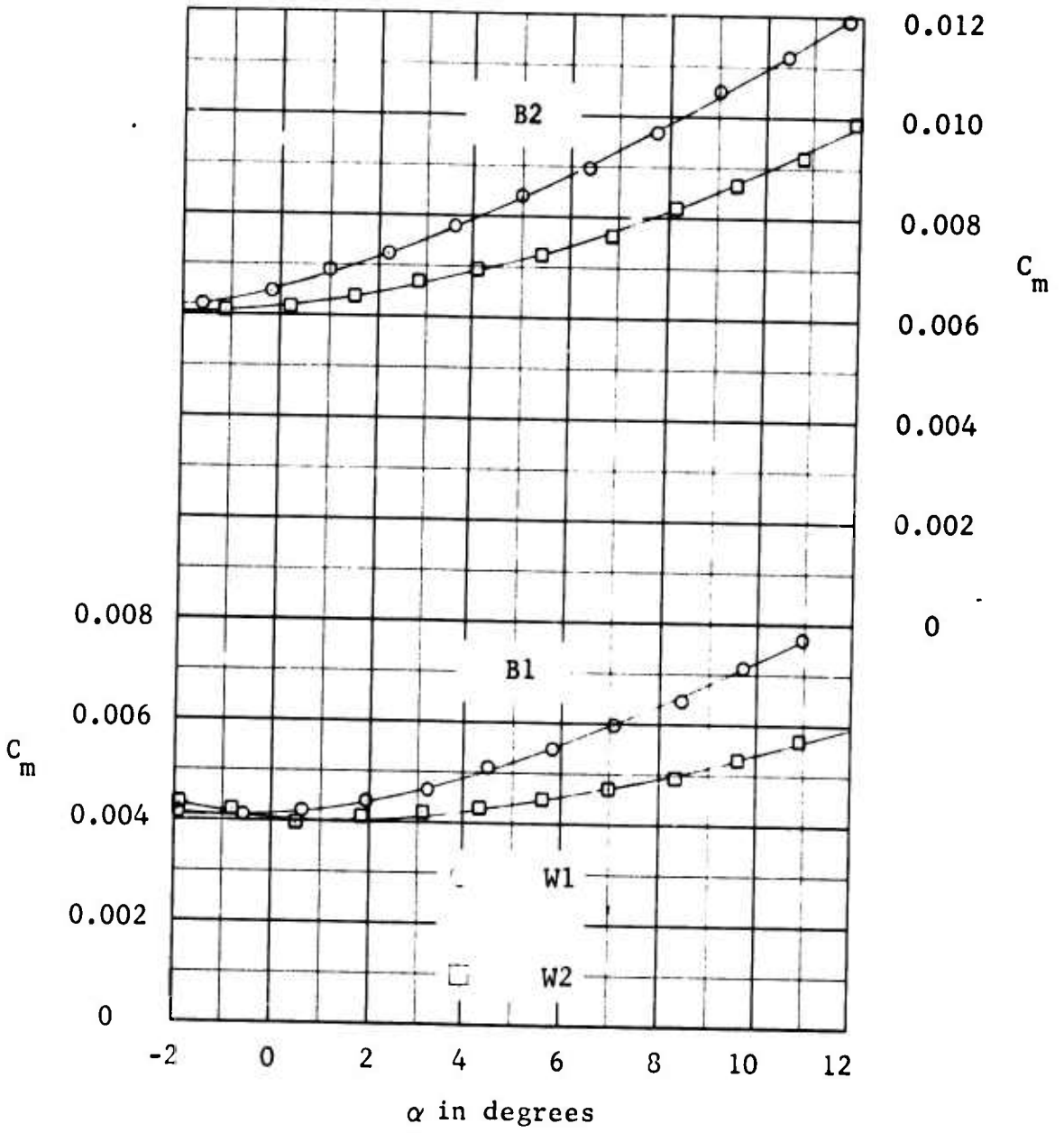

Figure 11 (Concluded)

(c) $\delta = -45°$

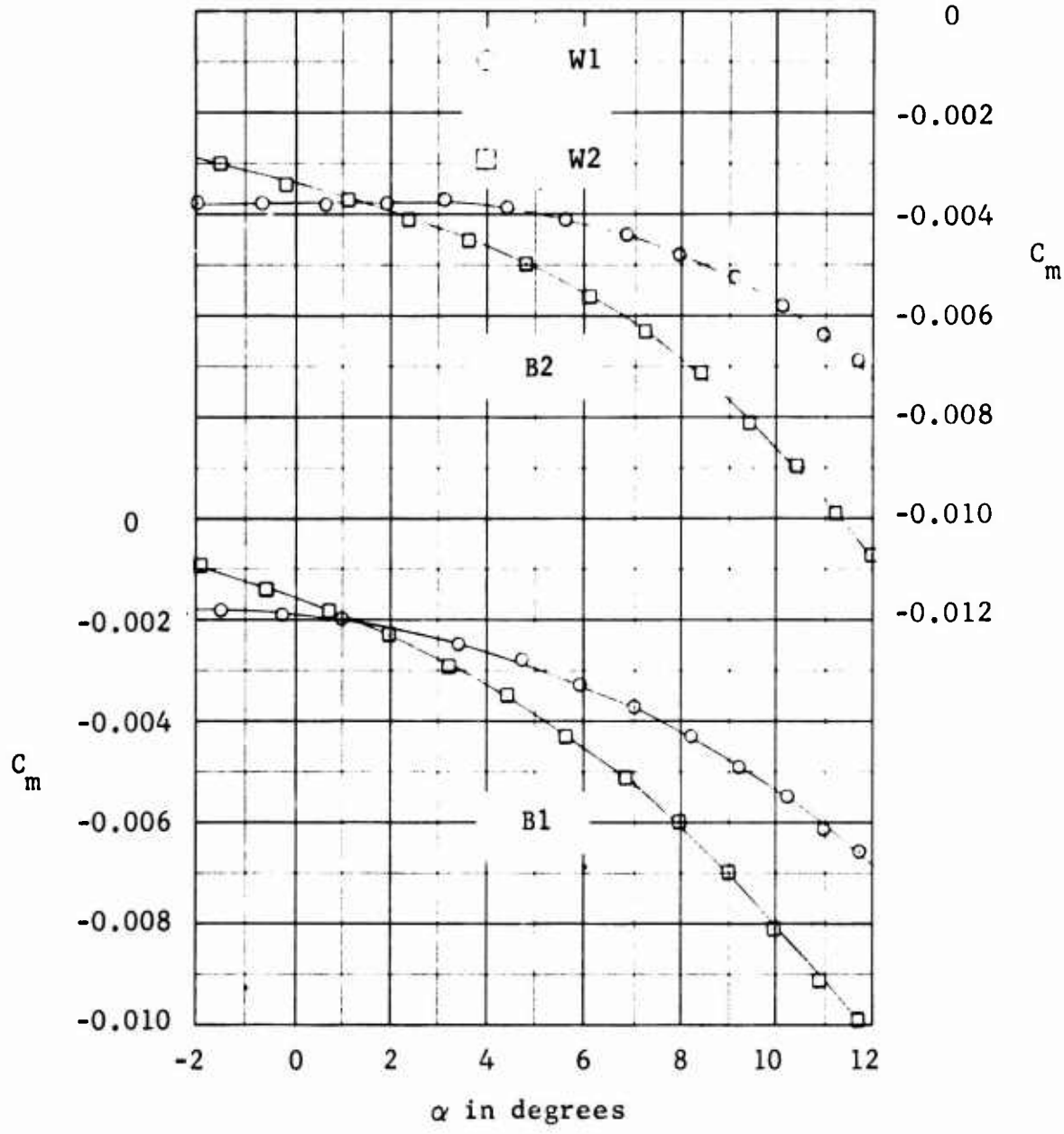

Figure 12 - Effects of Body Volume and Wing Planform on Pitching Moment Coefficient (Low-Wing Configurations)

(a) $\delta = 0°$

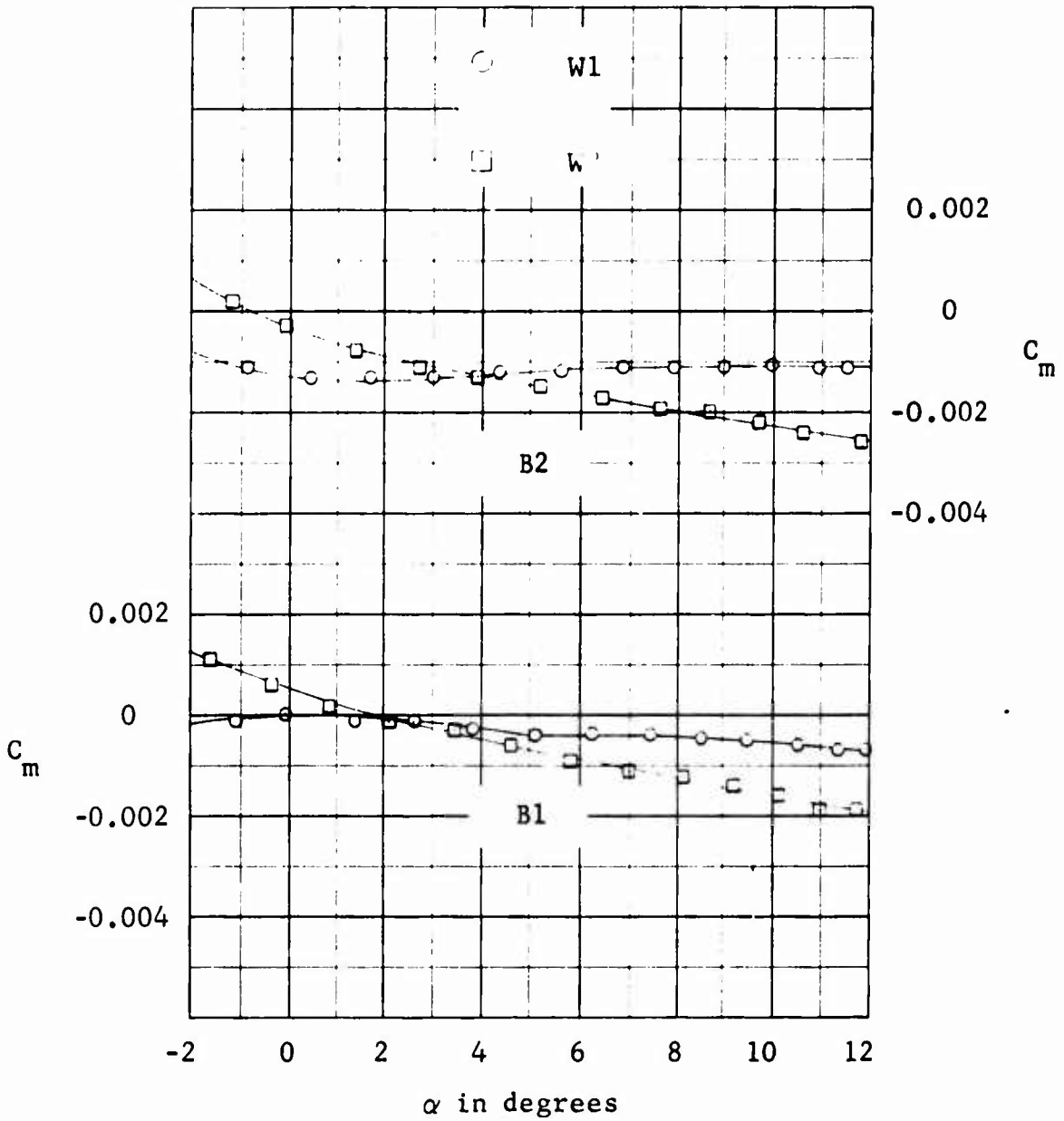

Figure 12 (Continued)

(b) $\delta = 45°$

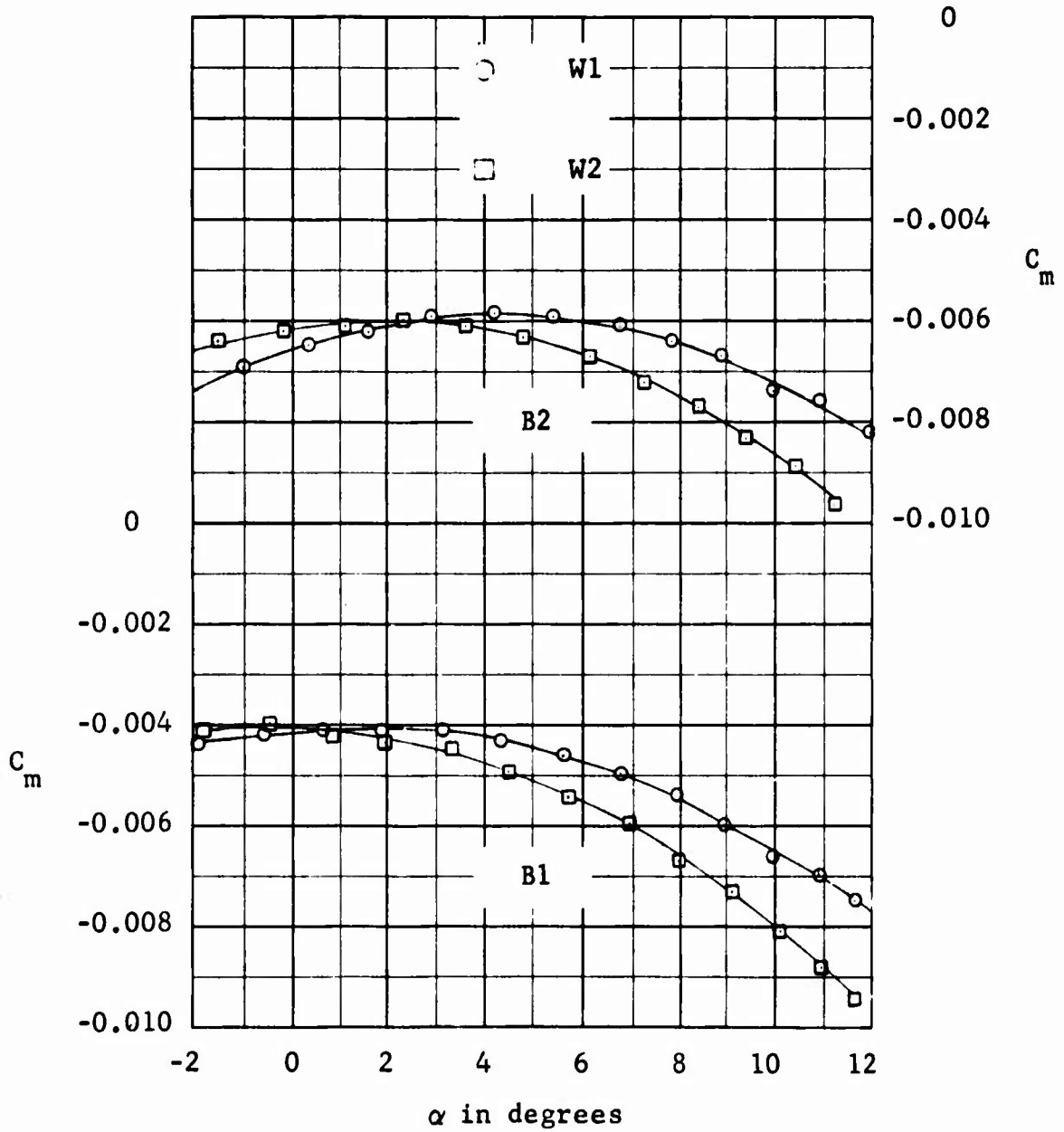

Figure 12 (Concluded)

(c) $\delta = -45°$

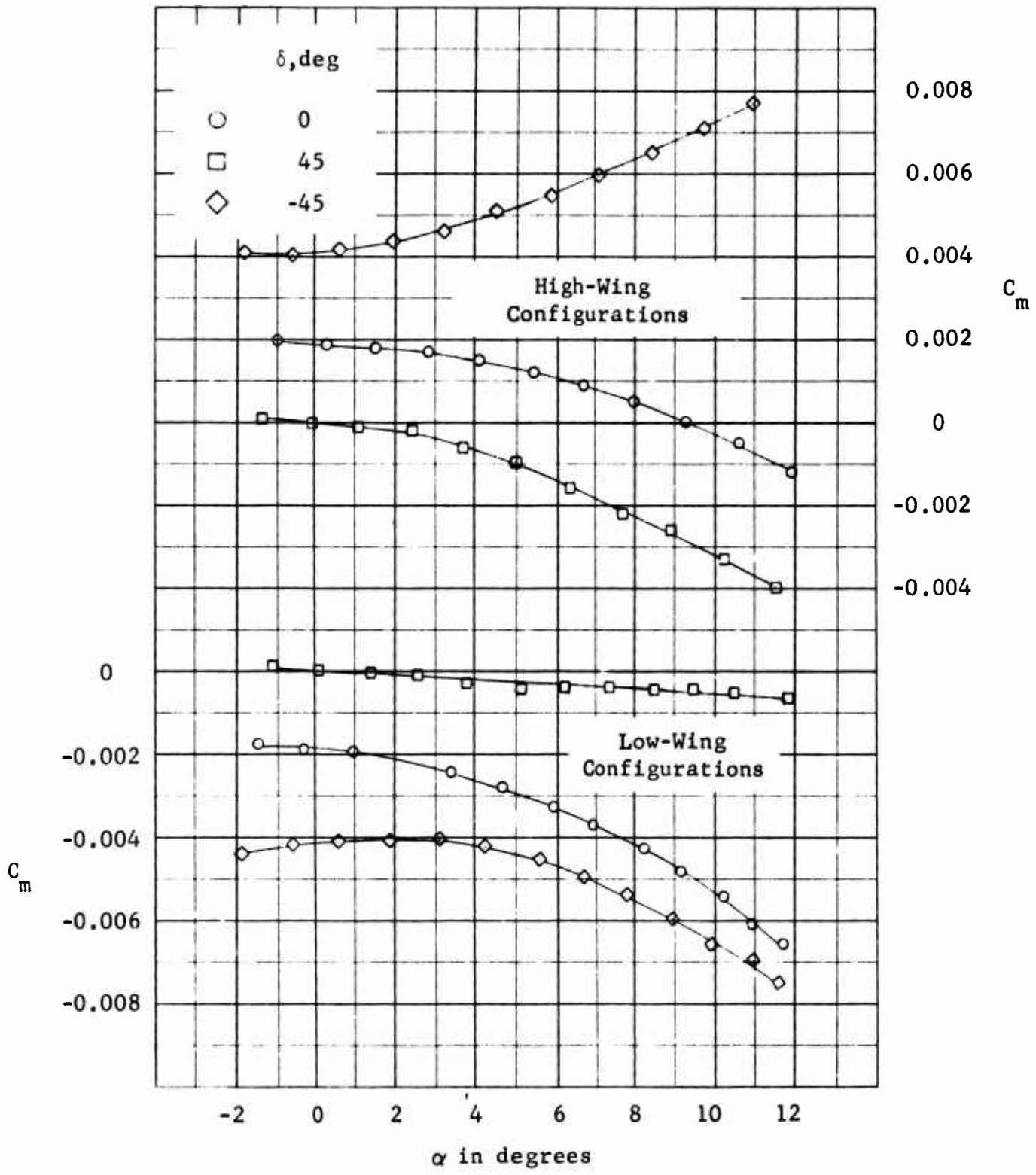

Figure 13 - Effects of Wing-Tip Dihedral and Vehicle Orientation on Pitching Moment Coefficient

(a) B1W1 Configurations

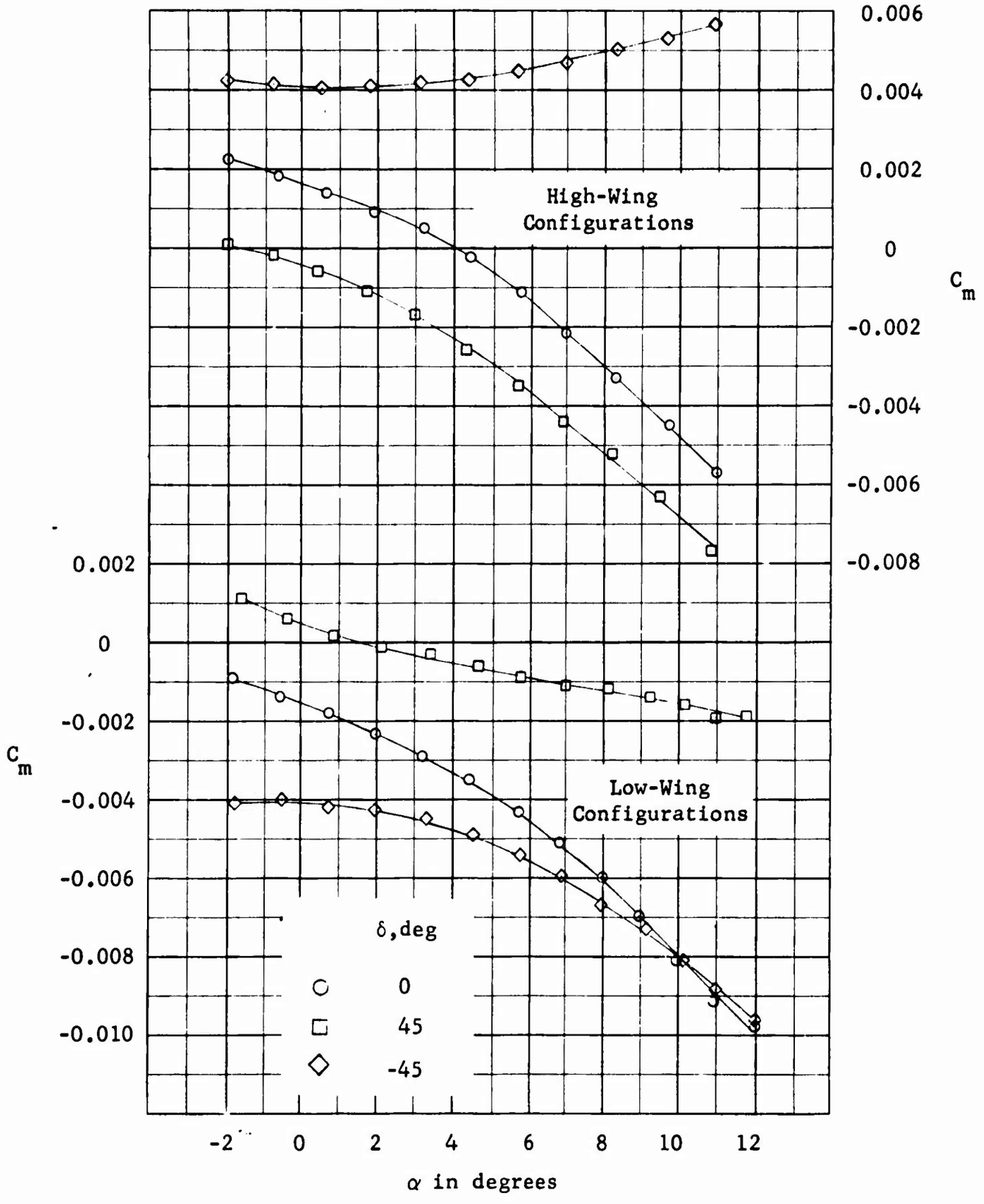

Figure 13 (Continued)

(b) B1W2 Configurations

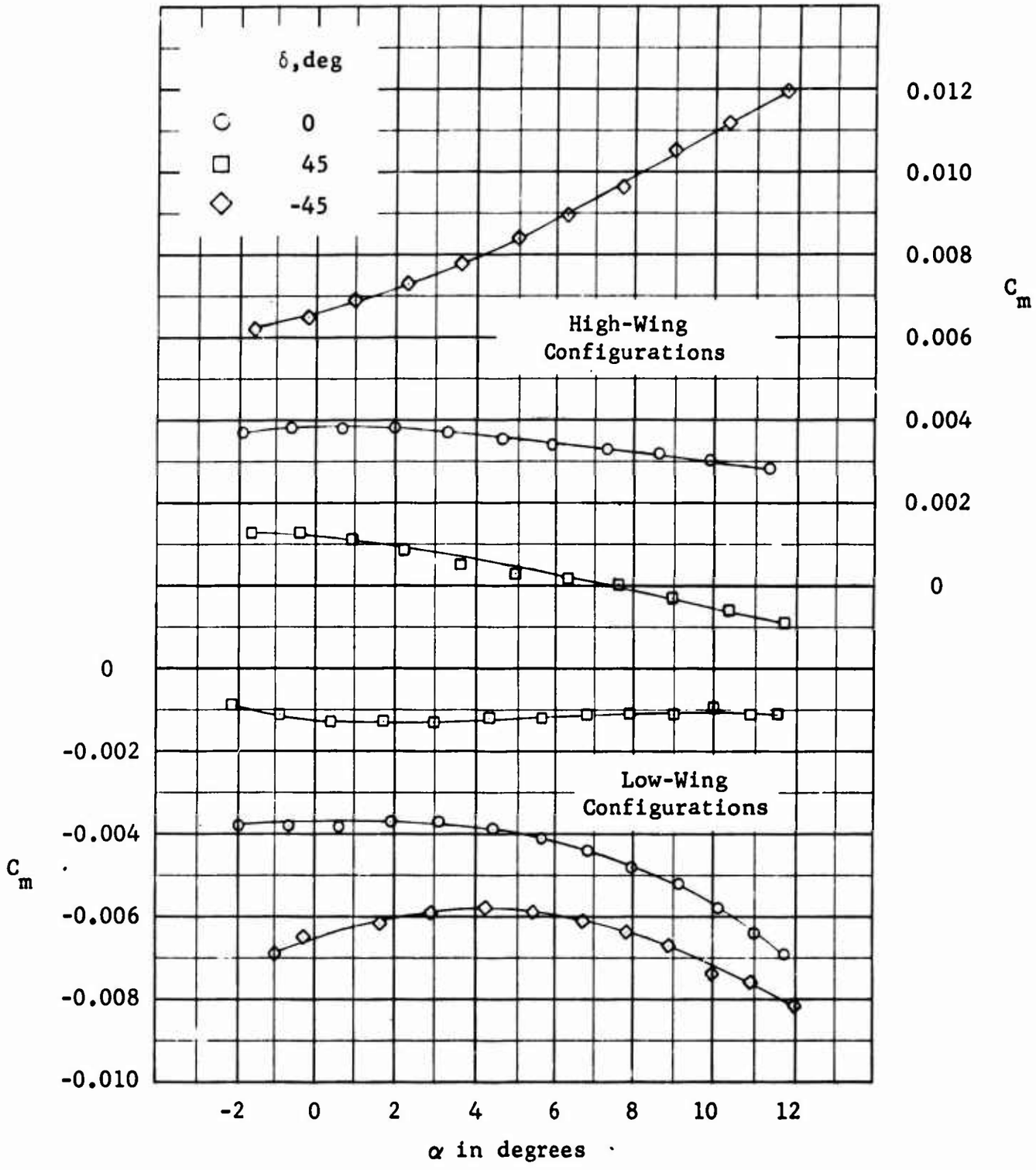

Figure 13 (Continued)

(c) B2W1 Configurations

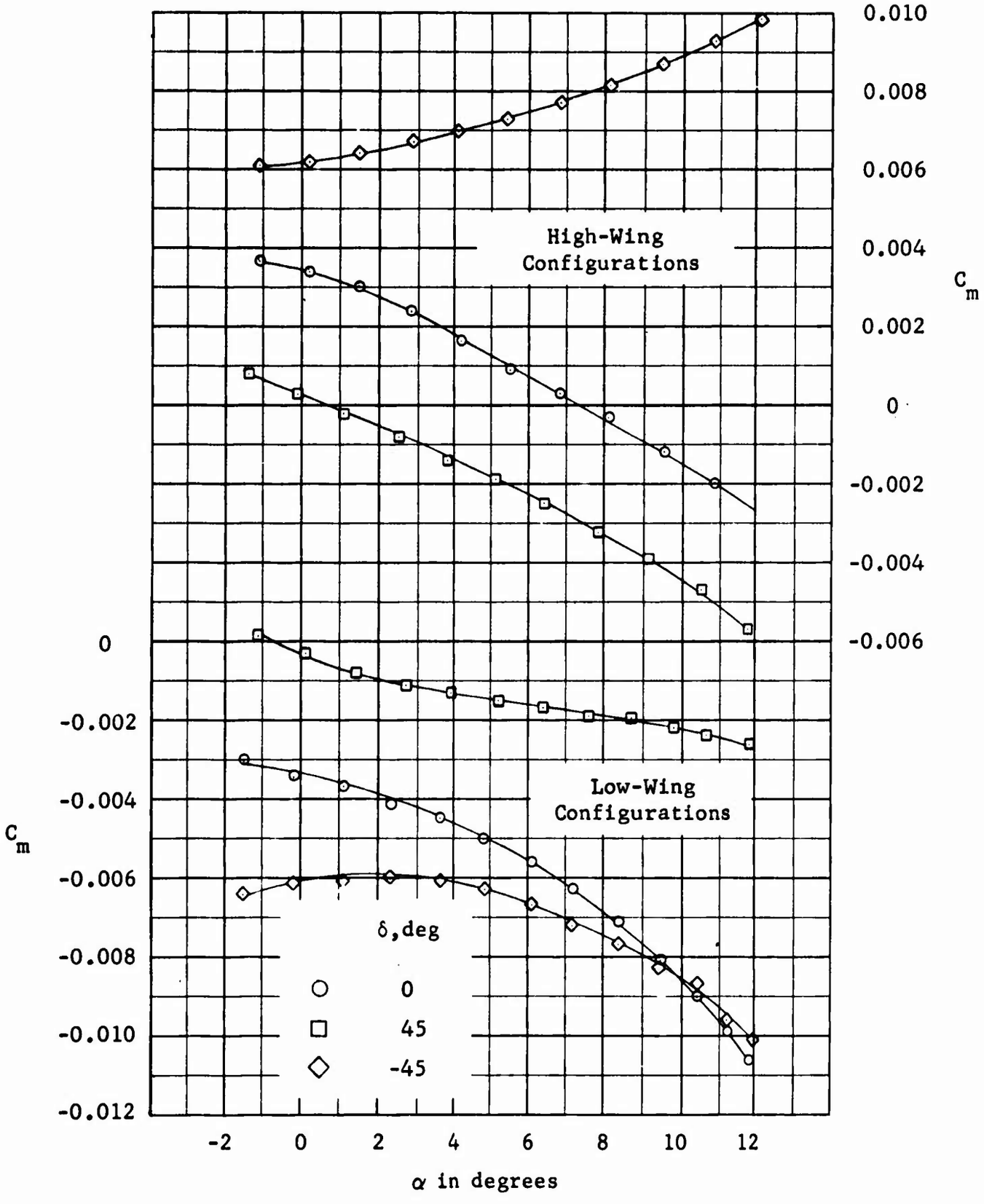

Figure 13 (Concluded)

(d) B2W2 Configurations

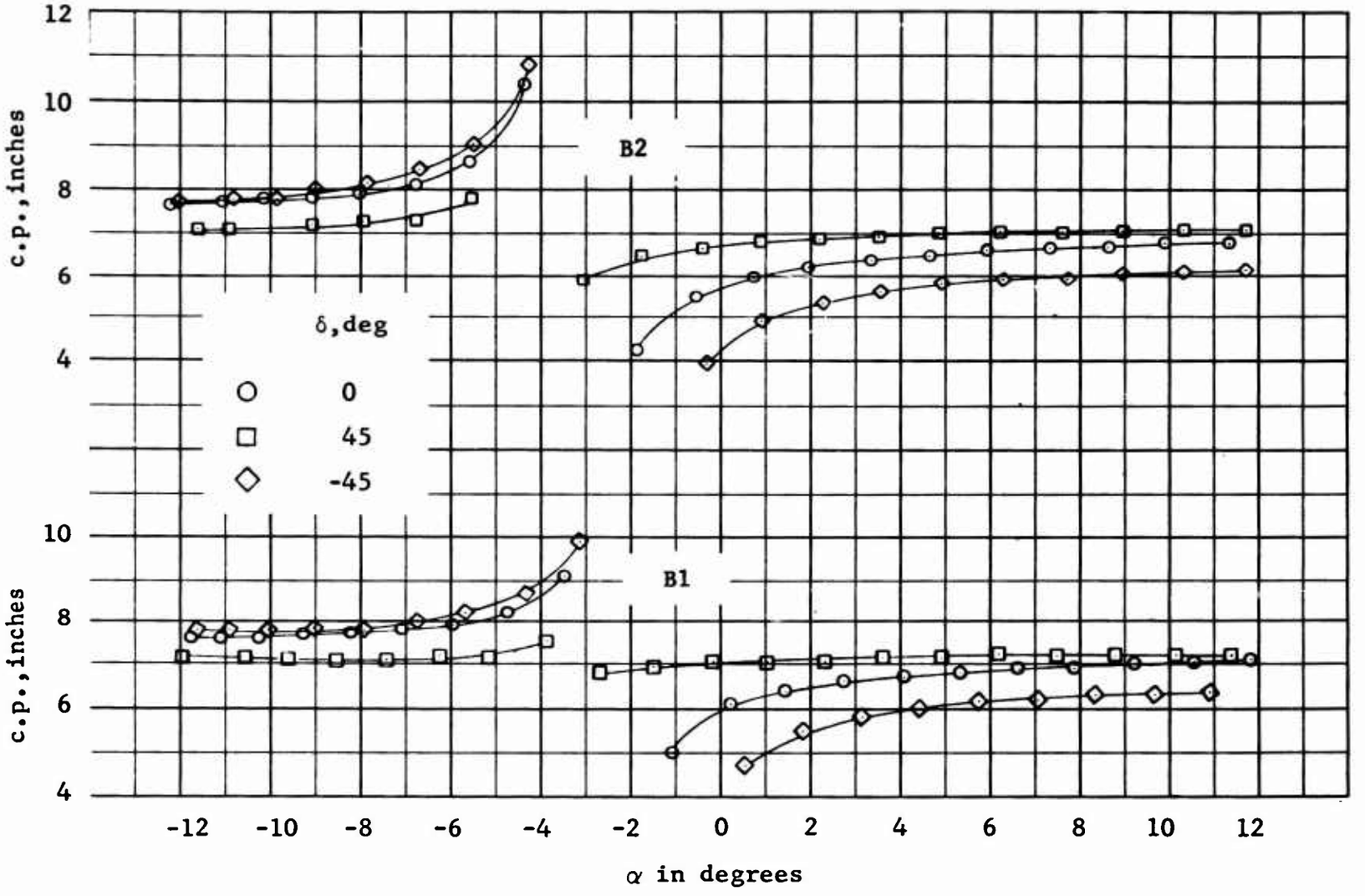

Figure 14 - Variation of Center of Pressure With Angle of Attack

(a) Series 1 Wings

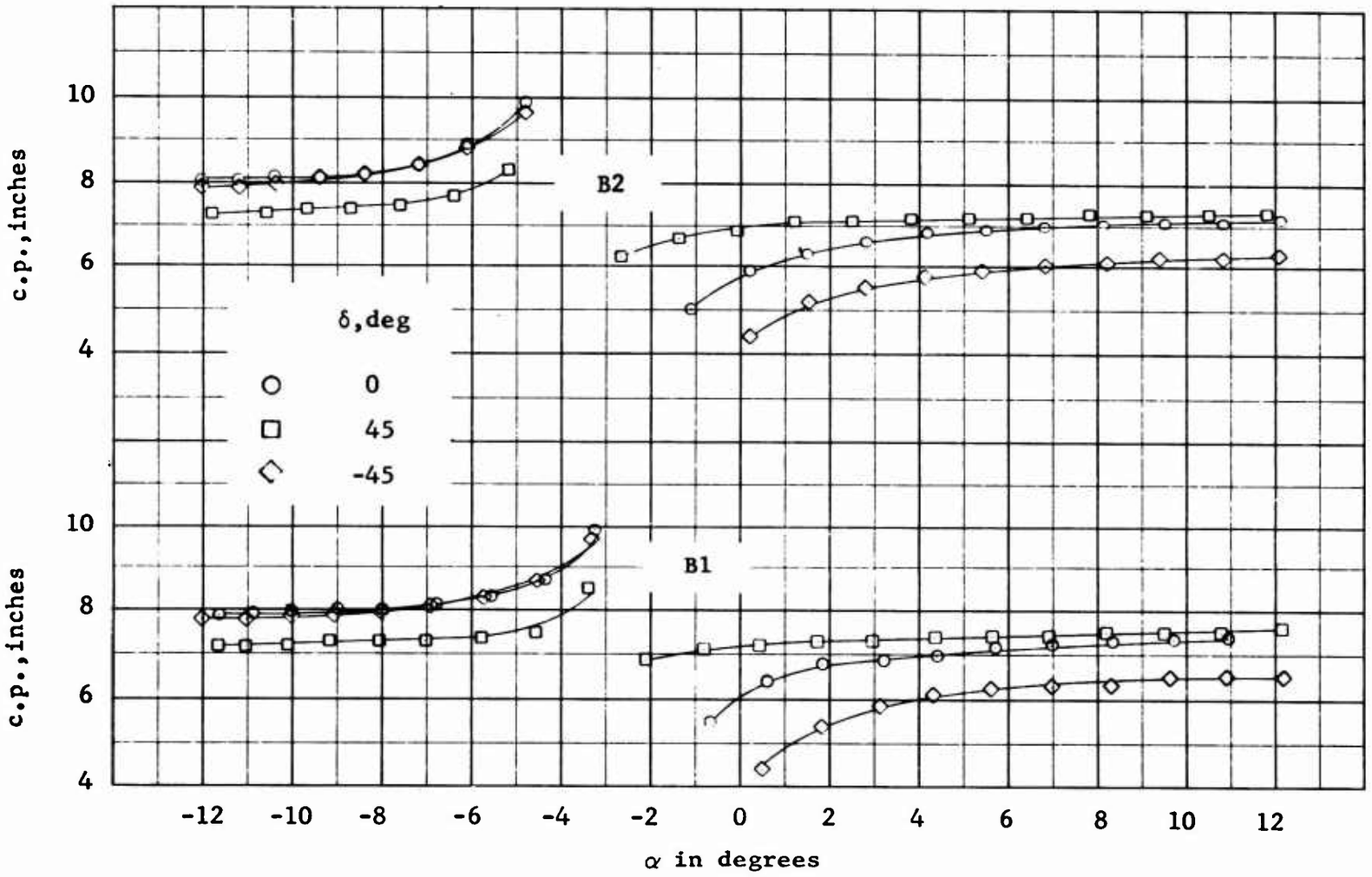

Figure 14 (Concluded)

(b) Series 2 Wings

Unclassified
Security Classification

DOCUMENT CONTROL DATA - R&D

(Security classification of title, body of abstract and indexing annotation must be entered when the overall report is classified)

1 ORIGINATING ACTIVITY *(Corporate author)* Aerodynamics Laboratory David Taylor Model Basin Washington, D. C. 20007	2a REPORT SECURITY CLASSIFICATION Unclassified 2b GROUP

3 REPORT TITLE

LONGITUDINAL AERODYNAMIC CHARACTERISTICS OF SEVERAL HYPERSONIC AIRCRAFT CONFIGURATIONS AT A MACH NUMBER OF 9.45

4 DESCRIPTIVE NOTES *(Type of report and inclusive dates)*

Formal Report

5 AUTHOR(S) *(Last name, first name, initial)*

Krouse, John R. and Ellis, Bertram K.

6 REPORT DATE	7a TOTAL NO OF PAGES	7b NO OF REFS
January 1966	40 [v]	7

8a CONTRACT OR GRANT NO.	9a ORIGINATOR'S REPORT NUMBER(S)
b PROJECT NO	Report 2153
c WEPTASK RAD 34B-001/440-1/F012-01-06	9b OTHER REPORT NO(S) *(Any other numbers that may be assigned this report)*
d	Aero Report 1099

10 AVAILABILITY/LIMITATION NOTICES

The distribution of this document is unlimited.

11 SUPPLEMENTARY NOTES	12 SPONSORING MILITARY ACTIVITY
	Bureau of Naval Weapons Department of the Navy Washington, D. C. 20360

13 ABSTRACT

Wind-tunnel tests were conducted at a Mach number of 9.45 to determine the longitudinal aerodynamic characteristics of several conceptual hypersonic aircraft configurations, consisting of various half-cone-cylinder bodies and double-delta wings. Effects of body volume, vehicle orientation, wing planform, and wing-tip dihedral were determined. In general, the lift-to-drag ratios of all high-wing configurations varied slightly over an angle-of-attack range of 0° to 12°, reaching a maximum value of 2.7 around 6°. On the other hand, the lift-to-drag ratios of all low-wing configurations increased continuously with increasing angle of attack, eventually reaching maximum values of roughly 3.0 near 12°. In all cases, fuselage base drag accounted for less than 4 percent of the total drag. For the arbitrarily chosen center-of-gravity location, all low-wing configurations were unstable, unbalanced, or both; whereas several high-wing configurations were both stable and balanced.

DD FORM 1 JAN 64 1473

Unclassified
Security Classification

14. KEY WORDS	LINK A		LINK B		LINK C	
	ROLE	WT	ROLE	WT	ROLE	WT
Hypersonic Aircraft						
Aerodynamic Forces						
Aerodynamic Efficiency						
Longitudinal Stability						
Static Stability						

INSTRUCTIONS

1. ORIGINATING ACTIVITY: Enter the name and address of the contractor, subcontractor, grantee, Department of Defense activity or other organization *(corporate author)* issuing the report.

2a. REPORT SECURITY CLASSIFICATION: Enter the overall security classification of the report. Indicate whether "Restricted Data" is included. Marking is to be in accordance with appropriate security regulations.

2b. GROUP: Automatic downgrading is specified in DoD Directive 5200.10 and Armed Forces Industrial Manual. Enter the group number. Also, when applicable, show that optional markings have been used for Group 3 and Group 4 as authorized.

3. REPORT TITLE: Enter the complete report title in all capital letters. Titles in all cases should be unclassified. If a meaningful title cannot be selected without classification, show title classification in all capitals in parenthesis immediately following the title.

4. DESCRIPTIVE NOTES: If appropriate, enter the type of report, e.g., interim, progress, summary, annual, or final. Give the inclusive dates when a specific reporting period is covered.

5. AUTHOR(S): Enter the name(s) of author(s) as shown on or in the report. Enter last name, first name, middle initial. If military, show rank and branch of service. The name of the principal author is an absolute minimum requirement.

6. REPORT DATE: Enter the date of the report as day, month, year; or month, year. If more than one date appears on the report, use date of publication.

7a. TOTAL NUMBER OF PAGES: The total page count should follow normal pagination procedures, i.e., enter the number of pages containing information.

7b. NUMBER OF REFERENCES: Enter the total number of references cited in the report.

8a. CONTRACT OR GRANT NUMBER: If appropriate, enter the applicable number of the contract or grant under which the report was written.

8b, 8c, & 8d. PROJECT NUMBER: Enter the appropriate military department identification, such as project number, subproject number, system numbers, task number, etc.

9a. ORIGINATOR'S REPORT NUMBER(S): Enter the official report number by which the document will be identified and controlled by the originating activity. This number must be unique to this report.

9b. OTHER REPORT NUMBER(S): If the report has been assigned any other report numbers *(either by the originator or by the sponsor)*, also enter this number(s).

10. AVAILABILITY/LIMITATION NOTICES: Enter any limitations on further dissemination of the report, other than those imposed by security classification, using standard statements such as:

(1) "Qualified requesters may obtain copies of this report from DDC."

(2) "Foreign announcement and dissemination of this report by DDC is not authorized."

(3) "U. S. Government agencies may obtain copies of this report directly from DDC. Other qualified DDC users shall request through _____."

(4) "U. S. military agencies may obtain copies of this report directly from DDC. Other qualified users shall request through _____."

(5) "All distribution of this report is controlled. Qualified DDC users shall request through _____."

If the report has been furnished to the Office of Technical Services, Department of Commerce, for sale to the public, indicate this fact and enter the price, if known.

11. SUPPLEMENTARY NOTES: Use for additional explanatory notes.

12. SPONSORING MILITARY ACTIVITY: Enter the name of the departmental project office or laboratory sponsoring *(paying for)* the research and development. Include address.

13. ABSTRACT: Enter an abstract giving a brief and factual summary of the document indicative of the report, even though it may also appear elsewhere in the body of the technical report. If additional space is required, a continuation sheet shall be attached.

It is highly desirable that the abstract of classified reports be unclassified. Each paragraph of the abstract shall end with an indication of the military security classification of the information in the paragraph, represented as *(TS), (S), (C), or (U)*.

There is no limitation on the length of the abstract. However, the suggested length is from 150 to 225 words.

14. KEY WORDS: Key words are technically meaningful terms or short phrases that characterize a report and may be used as index entries for cataloging the report. Key words must be selected so that no security classification is required. Identifiers, such as equipment model designation, trade name, military project code name, geographic location, may be used as key words but will be followed by an indication of technical context. The assignment of links, roles, and weights is optional.